Review Article

Insights into microscopic fabrication, macroscopic forms and biomedical applications of alginate composite gel containing metal-organic frameworks

Yuanke Zhang[a], Lvyao Yang[a], Min Zhou[a], Yanhua Mou[b,*], Dongmei Wang[c,*], Peng Zhang[a,*]

[a] Wuya College of Innovation, Shenyang Pharmaceutical University, No. 103, Wenhua Road, Shenyang 110016, China
[b] College of Life Sciences and Biopharmaceutics, Shenyang Pharmaceutical University, No. 103, Wenhua Road, Shenyang 110016, China
[c] College of Pharmacy, Shenyang Pharmaceutical University, No. 103, Wenhua Road, Shenyang 110016, China

ABSTRACT

Overcoming the poor physicochemical properties of pure alginate gel and the inherent shortcomings of pure metal-organic framework (MOF), alginate/MOF composite gel has captured the interest of many researchers as a tunable platform with high stability, controllable pore structure, and enhanced biological activity. Interestingly, different from the traditional organic or inorganic nanofillers physically trapped or chemically linked within neTtworks, MOFs crystals can not only be dispersed by crosslinking polymerization, but also support self-assembly in-situ under the help of chelating cations with alginate. The latter is influenced by multiple factors and may involve some complex mechanisms of action, which is also a topic discussed deeply in this article while summarizing different preparation routes. Furthermore, various physical and chemical levels of improvement strategies and available macroforms are summarized oriented towards obtaining composite gel with ideal performance. Finally, the application status of this composite system in drug delivery, wound healing and other biomedical fields is further discussed. And the current limitations and future development directions are shed light simultaneously, which may provide guidance for the vigorous development of these composite systems.

1. Introduction

Hydrogel, a kind of soft, water-swollen hydrophilic three-dimensional (3D) network structure formed by crosslinking and polymerization of natural or synthetic biological macromolecules, can be made into rigid gel beads, porous aerogels or flexible gel membranes and so on after further processing [1,2]. Interestingly, they have acted as promising platforms for drug delivery, tissue engineering, flexible
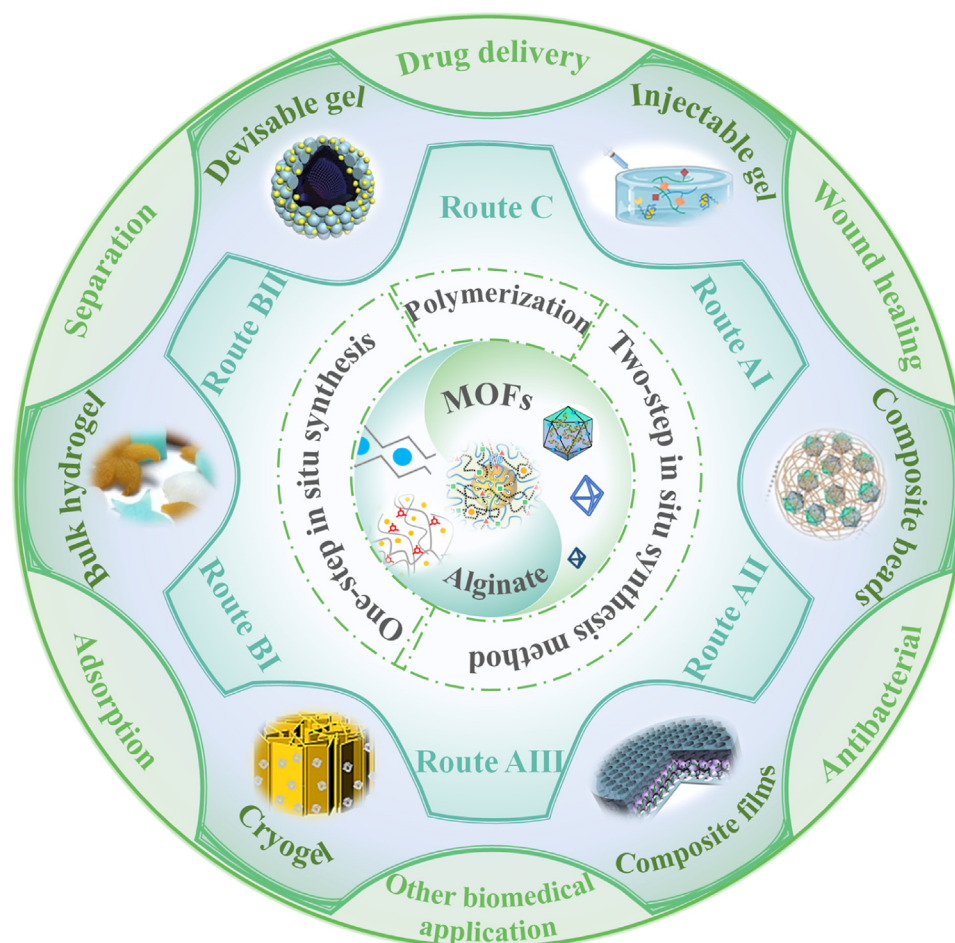
Scheme 1 – The manufacturing routes, application forms and applications of MOFs@Alg composite gel.

electronics, soft actuators, and catalysis, et al. [3-6]. Among them, natural polymer substances are more popular due to their wide sources, high biocompatibility, and low toxicity. Sodium alginate (SA) is a natural anionic polysaccharide with excellent biocompatibility, high chemical stability, strong gelation, and easy functionalization. Structurally, SA is a block-copolymer consisting of β-D-mannuronic acid (M) and α-L-glucuronic acid (G) (Fig. 1**A**) [7,8]. Furthermore, the different combinations of G and M form three different block types, namely M- blocks with continuous M residues, G- blocks with continuous G residues, and MG- blocks with random alternating M and G residues, as shown in the (Fig. 1**B**) [9]. Based on the rich carboxyl groups on the SA chain, the "egg-box" model mechanism of hydrogels with open lattice networks induced by Ca^{2+} has been widely recognized [10]. Meanwhile, more types of divalent, trivalent, and even monovalent cations have been successfully used to crosslink SA for different microstructures [11]. However, it should be noted that although the crosslinking mechanism between various divalent cations and SA is often interpreted as the formation of the "egg-box" model, ionic gelling is the result of the joint action of nonspecific electrostatic interaction and oxygen atom coordination drive, so they have different affinity with three types blocks of SA chains [11,12]. G-blocks can form complete "egg-box" structures as crosslink

point, while MG- blocks tends to form a semi one and M-blocks can only be loosely fixed ions through electrostatic or coordination interactions unable to contribute crosslinking (Fig. 1**C**). Therefore, the characteristics of gel mainly depend on the ratio of G/M in SA and ion type, while the former is only related to the source of SA [11,13].

Besides, the 3D structure of alginate (Alg) will collapse during the dehydration process, resulting in surface cracks, insufficient mechanical strength, and tensile properties, greatly limiting its application [14,15]. Fortunately, as a good carrier material, the abundant hydroxyl and carboxyl groups rich in its surface can provide effective binding sites for some functional materials. It can inhibit the aggregation of nanomaterials and improve material effectiveness, while also achieving enhanced physical and chemical properties, making it a very promising multifunctional composite platform. Among them, metal-organic frameworks (MOFs), a kind of porous inorganic–organic hybrid crystals with extending 2D or 3D coordination networks, have been widely acted as hydrogel fillers for various applications [16,17]. Selectable metastable coordination bonds support their use as reservoirs for metal ion or organic ligand release; the ordered porous structure, easy to functionalize structure, and abundant active sites on the surface allow them to achieve effective drug loading or act as various types of adsorbents; special metal nodes,
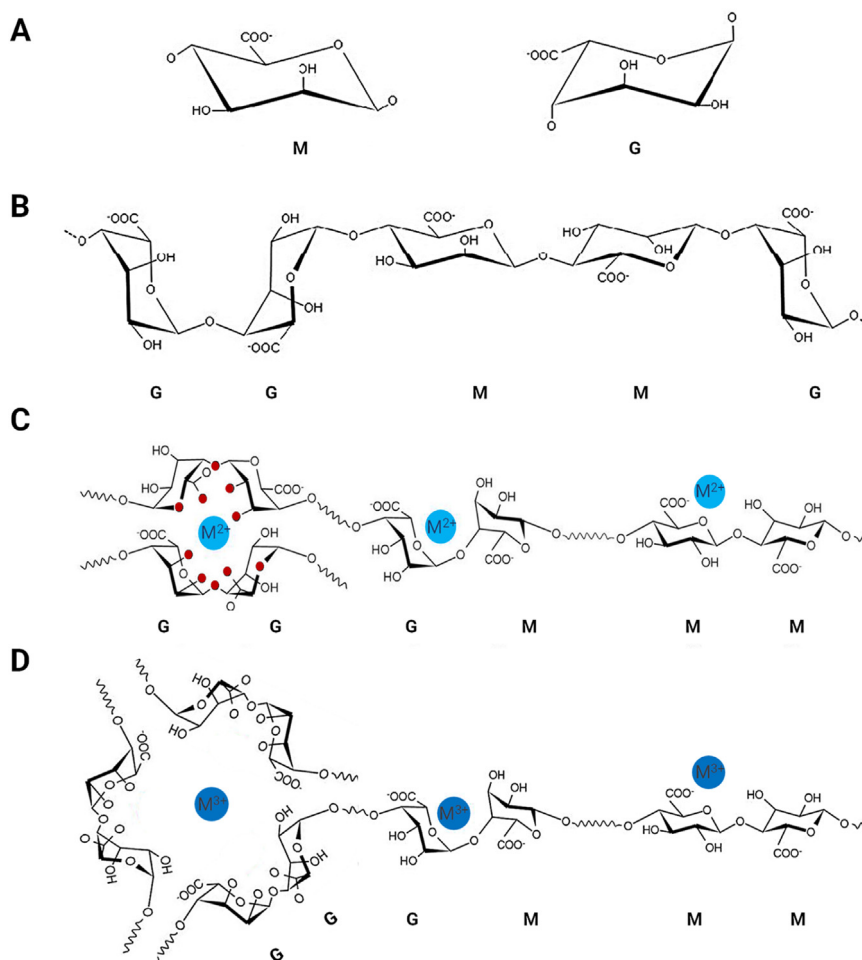
Fig. 1 – (A) The structures of β-D-mannuronic acid (M) and α-L-glucuronic acid (G). (B) Interconnection method of M and G residues. (C) Some binding sites of divalent cations and SA, with red indicating possible oxygen atom coordination sites. (D) Some binding sites of trivalent cations and SA. Only the G- blocks can form interchain crosslinking.

ligands, or ordered connection sequences may also endow them with catalytic activity, photo activity, heat generation, or fluorescence emission capabilities [18-22]. However, pure MOFs are powdery solids with defects such as poor stability, easy aggregation, uneven size distribution, and low biological safety, greatly limiting their application range. Therefore, using biopolymers as templates for self-assembly, coating, or encapsulating them through crosslinking polymerization is a very popular approach [23]. At the same time, based on the special ion induced gel mechanism of SA, the -COOH functionalized metal ions are highly dispersed, which can further drive the self-assembly process of subsequent MOFs, and its formation depends on the Ostwald ripening process [24]. Due to the viscosity of the solution and the steric hindrance of the chain, MOF crystals will not overgrow, and their size and distribution will also tend to be homogenized. From a microscopic perspective, due to the presence of abundant carboxyl groups around metal ions, the polarized surface of MOFs particles can serve as effective adhesives and excellent fillers to enhance the toughness and mechanical properties of Alg, manifested in improved pore structure

[25,26]. Compared to pure MOFs, the MOFs containing alginate composite gel (MOFs@Alg) seems to have higher loading capacity, more controllable drug release, delayed immune system clearance and a wider range of application [9,27-29]. In addition, different metal nodes, crosslinking ions, organic ligands, packaging strategies, and gel manufacturing methods will make MOFs@Alg with different structural characteristics and mechanical properties. Furthermore, through reasonable design, MOFs@Alg may display ideal pore size characteristics, stable and controllable macroscopic shape, enhanced biological activity, improved bioavailability, and excellent recyclability [30,31]. The advantages of MOFs@Alg are summarized in Table 1.

Oriented towards the excellent performance of MOFs@Alg, this paper will start with three encapsulation strategies, and deeply analyze the influence of different cations on the microstructure of the Alg gel network and MOF containing composites simultaneously to help readers understand their formation mechanism fundamentally. Furthermore, new improvement strategies are introduced from the level of polymers and MOFs, and ideas are provided for a more

Table 1 – Performance comparison of MOFs, Alg and MOFs@Alg.

Entry	MOFs	Alg	MOFs@Alg
Stability	bad	stable	stable
Biocompatibility	Determined by metal ions and ligands	Excellent	Excellent
Mechanical properties	Bad	Bad	Improved
Aperture	Determined by ligand size	Adjustable	Adjustable
Microforms	Powder	Diverse	Diverse
Application scopes	Limited	Wide	Wide
Enzyme-like activities	Majority	None	Determined by MOFs
Antibacterial activity	Wide	None	Wide
Deformability	none	Adjustable	Adjustable
Drug loading capacity	Low	Flexible	Flexible
Drug release mode	Single	Single	Composite
pH-responsive	Sectional	Yes	
Adsorption capacity	Excellent	None	Excellent

ideal composite platform in combination with a variety of available composite gel shapes. Finally, the focus will turn on introducing MOFs@Alg applications in the fields of drug delivery, antibacterial, wound healing and other biomedical fields. We hope to open up a broader path for the combination of MOFs and Alg through this systematic review.

2. Preparation methods and influencing factors of MOF@Alg

2.1. In situ synthesis method

Based on whether organic ligands and metal ions are added simultaneously, in-situ synthesis methods can be divided into one-step and two-step methods. Wherein, the two-step one is more often, where SA coordinates with metal ions before mediating the self-assembly of MOFs.

2.1.1. Two-step in situ synthesis method
After contacting a suitable ligand under certain conditions, the chelated metal ions in Alg can bind to the ligand so mediate the formation of a large number of MOF nuclei, named ligand-diffusion in-situ generation (Route AI and AII). The metal ions used for crosslinking SA and inducing nucleation can be the same or different [32-35]. Different ions for in-situ generation means that one is mainly for crosslinking and the other mainly applied for nucleation, as shown in Route AI (Fig. 3). Currently, there are two routes for crosslinking and synthesis using different ions. The first method is to add Alg generated by crosslinking with another metal ion during the MOF synthesis process. This method was improved by the traditional hydrothermal method to effectively generate MOF-525 (Zr) in situ in Cu-Alg [33]. Specifically, benzoic acid and $ZrOCl_2 \cdot 8H_2O$ were ultrasonically mixed and then heated at 353 K for 2 h. After natural cooling to room temperature, an appropriate amount of ligand and Cu-Alg were added to react for 24 h at 353 K. Another method is basically the same as the route of crosslinking and synthesis using the same ion, which is to directly disperse Alg in the precursor solution to prepare MOF. However, it is worth noting that the complexation between the metal ions used in the

first step and the Alg unit should be easily dissociated to allow for subsequent exchange of other metal ions, such as Li^+ [32]. By contrast, using the same type of ion as a node for MOF and Alg seems more common (Route AII) (Fig. 3). Among them, the novel MOF with different graded pores will cause a large number of Alg chains to entangle or crosslink on its surface, coupled with the chelation effect of Alg on metal ions, which in turn will limit the growth of MOF nuclei and prevent them from forming large particles [36,37]. At the same time, the successful modification of MOF increased the porosity of Alg [35]. However, the network structure crosslinked by metal ion in advance may hinder the diffusion amount and rate of organic ligands to some extent, especially inside the gel, where may not be able to accumulate enough concentration of ligands for MOFs crystals formation. Furthermore, as some of the metal ions involved in crosslinking leave the chelating sites to participate in crystal self-assembly, the composite material ultimately manifests as a smaller size compared to pure Alg [38,39]. Besides, the addition sequence of metal ions and organic ligands can also be reversed, that is, the mixed solution of SA and organic ligands is initially solidified by various crosslinking methods and subsequently immersed in a solution containing metal node ions to initiate MOF nucleation self-assembly, which is called metal ion diffusion in-situ generation method (Route AIII) (Fig. 3) [40,41]. This method is very beneficial for the formation of secondary crosslinking networks and maximally avoids the influence of the resistance on the diffusion of organic ligands into the gel after metal ion crosslinking of the first step, thus allowing the crystal nucleus to successfully grow inside the gel. Meanwhile, because the organic ligands cannot be fixed and coordinated in time, the internal ligands will gradually seep out and the metal ions in the external solution will gradually diffuse to the interior of the gel, so that the ligands and metal ions will form concentration gradients from high to low and from low to high in the interior and surface of the gel, respectively. Therefore, the size of the nuclei formed on the external surface is small and dense, while the interior is large and loose. Furthermore, in virtue of the high controllability and uniformity of 3D printing, this method is more likely to generate MOFs crystal nuclei with controllable sizes in-situ [41]. Fig. 2**A** shows that the interpenetrating
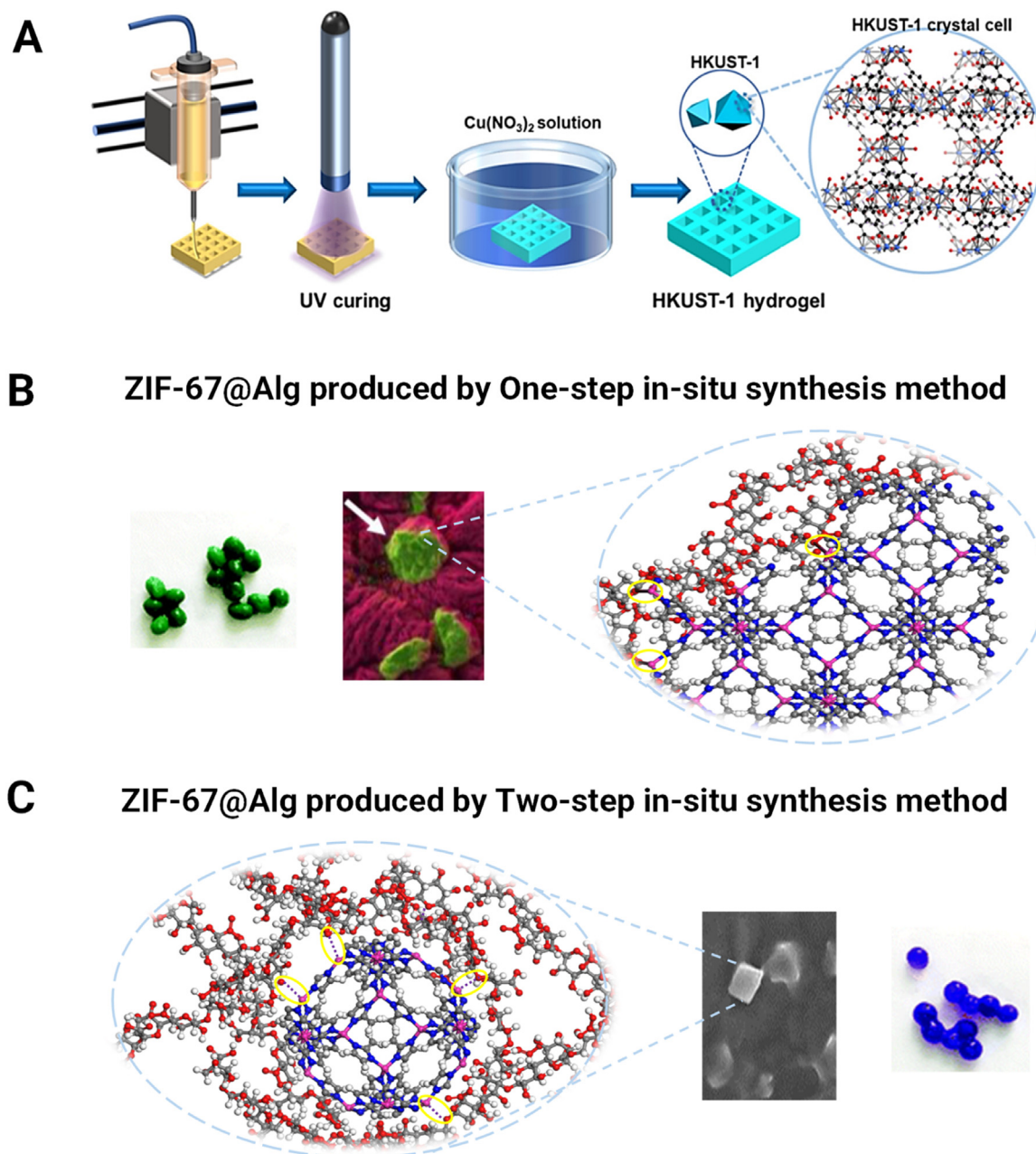
Fig. 2 – (A) Schematic showing the three critical steps in the 3D printing process including printing, UV curing, and ionic crosslinking. Reproduced from [41] with permission from American Chemical Society. **(B)** Co^{2+} simultaneously coordinated with the -COOH of SA and the N atom of 2-methylimidazole (2-Ml), forming a novel MOF-like structure, with the solid lines inside the yellow circle representing the coordination bond. **(C)** The standard ZIF-67 crystal structure was connected to the SA chain through non-bonding interactions, with the dashed lines inside the yellow circle indicating electrostatic interactions.

network (IPN) composite hydrogel containing MOF formed by UV crosslinking. There were corresponding photoinitiators and photocrosslinkable polymers in the precursor solution, which could effectively encapsulate the ligand while forming the initial shape of the gel.

2.1.2. One-step in situ synthesis method
Another method of in-situ synthesis is to simultaneously add organic ligands and metal ions into SA solution, while initiating crosslinking and assembly (Route BI and BII) (Fig. 3). Among them, the added metal ions can be different, one is only used for crosslinking, and the other act both of two effects at the same time. For example, dropped a mixed solution of SA/ carrageenan/ 2-Ml into a methanol solution of Zn^{2+} and Ca^{2+} to obtain composite beads incorporated with ZIF-8 (Zn) [26]. The electron microscopy image showed a uniform distribution of ZIF-8 particles without significant aggregation. However, compared to the two-step method, the newly
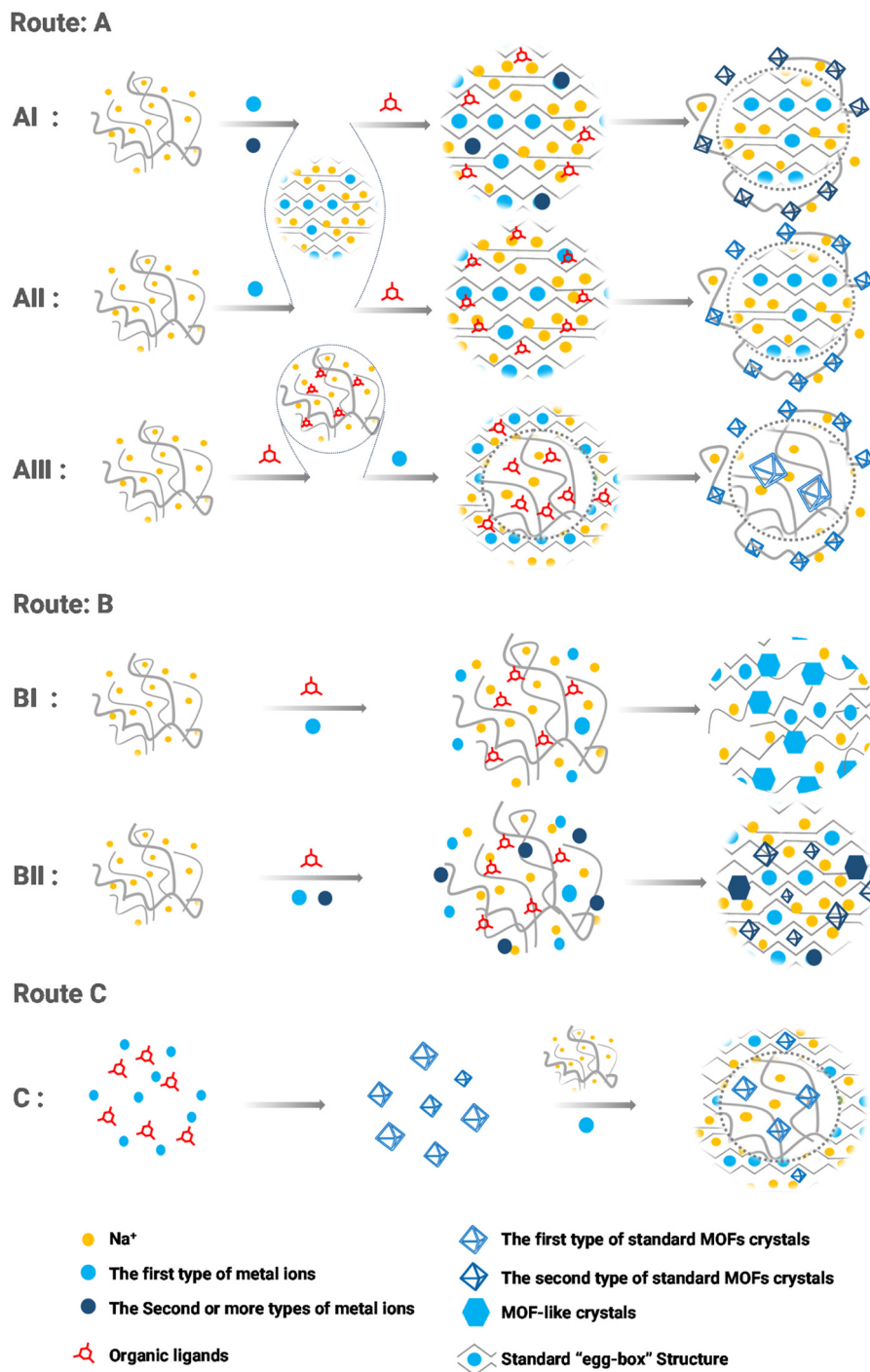
Fig. 3 – The preparation roadmap of MOFs@Alg composite gel. (A) The route diagram of the two step of synthesis method. Route AI and AII represent the two-step ligand diffusion in-situ generation methods involving crosslinking and nucleation of different and identical metal ions, respectively. In this way, MOFs crystals are mainly formed outside the gel, and the internal network structure remains. Route AIII represents the two-step ion diffusion in-situ generation method, which can induce the formation of large and small standard MOFs crystal structures inside and outside the gel respectively. (B) The route diagram of the one-step in-situ generation methods. Route BI and BII represent the one-step in-situ generation methods involving crosslinking and nucleation of the same and different metal ions, respectively. The former forms MOF-like crystals in the gel because metal ions participate in both crosslinking and nucleation simultaneously. Nevertheless, the latter one helps to maintain the original network structure of the gel to a certain extent because of the addition of additional crosslinked nodes, on the premise that SA has a higher affinity for additional ones. (C) Schematic diagram of crosslinking polymerization method. Among them, standard MOFs crystals can be evenly distributed inside and outside the gel, and the external gel is more crosslinked.

generated MOF nucleus produced by one-step manifested a MOF like structure in Alg, because them were formed by the simultaneous chelation of metal ions with SA and organic ligands. The ZIF-67@Alg synthesized by one-step method was green and had a rough microstructure, compared to the two-step synthesis with a blue appearance and relatively smooth microstructure (Fig. 2B and 2C) [42]. Because the hydrogel prepared by one-step method had significantly stronger -OH and -COOH groups, and was easy to form intramolecular hydrogen bonds, resulting in stronger interaction between Alg and MOF [42]. However, perhaps due to the limitations of this irregular MOF-like structure in terms of application, this method has been less reported. Interestingly, Vahed et al. prepared ZIF-8 incorporated Alg using a one pot ball milling method and the perfect original crystal structure was retained [31]. Specifically, the solid mixture of 2-Ml/ zinc acetate/SA formed self-assembly by ball milling at room temperature of 28 HZ for 1 h, which method avoided the use of organic solvents while preserving the crystal structure.

2.1.3.　Factors affecting the in situ generation of MOFs

There is a study that had explored the effects of reaction temperature, reaction time, and amount of Alg on experimental results in organic ligand solutions through orthogonal experiments [34]. Since the ultimate goal of this study was to fabricate the composite particles of magnesium hydroxide (MH) coated with MOF-incorporated Alg gel for preferable flame retardancy, the experiment also explored the influence of MH dosage on the results and took the limiting oxygen index (LOI) as the evaluation index. The final results indicated that the amount of Alg, reaction time, MH amount, and reaction temperature all have an impact on the indicators. In addition, different solution systems can also affect the in-situ generation of MOFs.

2.1.3.1. *The ALG and reaction time*　Due to the coordination crosslinking of SA involves diverse microcosmic mechanisms and the Alg indirectly represents the amount, availability, and coordination ability of metal ions in the MOF synthesis reaction, all of which will impact in-situ generation. What is more, due to the different chelating abilities of various types or oxidized states metal ions on Alg and organic ligands, newborn MOFs@Alg ultimately will exhibit different distribution states of cores and physicochemical properties [11,43,44].

Firstly, different types of metal ions affect the loading and nucleation of metal ions due to their different crosslinking methods and affinities with SA chains. Both nonspecific electrostatic interaction and oxygen atom coordination can mediate ion induced gelation [12]. The affinities between divalent metal ions and SA were arranged in descending order as follows: $Pb^{2+} > Cu^{2+} > Cd^{2+} > Ba^{2+} > Sr^{2+} > Ca^{2+} > Co^{2+}$, Ni^{2+}, $Zn^{2+} > Mn^{2+}$ [45,46]. Among them, Cu^{2+} with high affinity for SA can not only coordinate with the G-blocks to form a classic "egg-box" structure, but also support in complexing with the GM- and M- blocks. Its affinity is ten times higher than that of Ca^{2+}, which can bind with both G- and MG- blocks, thereby requiring less amount to induce Alg gelation [46,47]. When Cu^{2+} of high concentration (32 mmol/l) contacts with SA, coordination crosslinking can

occur rapidly within a few min, forming a dense and thick gel layer, thus preventing ions from further diffusing to form inner crosslinking [48]. That is to say, for divalent cations, the gelatinization rate is the key factor to control the gel uniformity, which is closely related to the ion concentration [48,49]. By contrast, Co^{2+} and Zn^{2+} with weaker affinity can only replace Na^+ in G- blocks, which is the only source of nucleation ions. With the formation of MOF crystal, the lack of crosslinking sites may lead to the dissociation of gel network [50]. In contrast, at suitable concentration of Cu^{2+} and sufficient crosslinking time, Na^+ can be completely replaced, while Cu^{2+} located at non-crosslinking points can serve as excellent nucleation sites. However, it is worth mentioning that at high metal concentration levels and long crosslinking times, almost all types of metal ions can form weak interactions with some MM- blocks, but the binding force is poor [51]. A typical example was that compared to the composite gel containing Fe or Al based on the same ligand 1,3,5-benzenetricarboxylicacid (H_3BTC) and manufacturing method, Cu-MOF (HKUST-1) @Cu-Alg had the best tensile properties and the polymer wall was compact and smooth, which could effectively improve the mechanical properties of the composite gel [36]. Part of the reason was the strong crosslinking performance of Cu^{2+}, and partly due to the relatively large pore size of HKUST-1 supporting more effective entanglement with the polymer. Although the chelation mechanism between Al^{3+} and SA had not been fully elucidated, it was also believed that Al^{3+} could coordinate with carboxylic groups containing uronic acids to form a three-dimensional structure like Fe^{3+} (Fig. 1D) [11]. Therefore, the hydrogel containing Fe-MOF (MIL-100 (Fe)) had the best compression performance, possibly owing to the most regular cavities like ice crystal inside networks. By contrast, because Al-MOF did not have crystal characteristics due to the inherent characteristics of non-transition metals, the properties of Al-MOF containing gel were not outstanding [39].

Next, metal ions with different valence states affect the microstructure of composite materials through coordination numbers. The study reported that under the same conditions, the growth of phosphate-MOF in Cu-Alg was uneven, while the growth in Al-Alg was uniform [39]. That was because the phosphate organic ligand N, N'-piperazine bis (methylene phosphonic acid) (N_2PMP) induced Cu oxidation state to change from Cu^{2+} to Cu^+ and Cu. These low-valence Cu had lower coordination numbers and affinity with carboxyl groups, resulting in the formation of new MOF nuclei accompanied by the rearrangement of the original "egg-box" structure, ultimately exhibiting an uneven distribution of MOF nuclei. What is more, metal ions with different valence states have different affinities with SA that affect the crosslinking and thus affect the formation of new nuclei. Both Fe^{2+} and Fe^{3+} have same coordination number of 6, but the coordination ability between Fe^{2+} and SA units decreases. Because Fe^{2+} is more inclined to bind neutral ligands containing N and S atoms compared to Fe^{3+}, which preferentially binds with carboxylate of uronic acid to induce the formation of 3D interconnected structure of Alg [52]. Therefore, when Fe^{3+} is reduced by the outside world, it will lead to the dissolution of Alg [44]. In addition, during the

subsequent nucleation process, the growth of Fe-MOF is more strictly restricted in the gelling network due to the retention of Fe^{3+} crosslinking sites, leading to the penetration of Alg chains into MOF pores, thus reducing the pores and surface area of the gel, which is similar to the Cu^{2+} [50,53].

2.1.3.2. *Temperature* Generally speaking, higher temperature endows the SA chain with higher thermal energy and extended conformation with reducing topological constraints, resulting in increasing grid size of the transient polymer network and lower solution viscosity [54]. Meanwhile, the leaching of ions and ligands within carriers will increase with the up of reaction temperature due to the faster molecular motion and reduced solution viscosity, which is conducive to the formation of MOF nuclei [23]. However, different metal ions will exhibit the highest coordination ability and stability with diverse organic ligands at specific temperatures. What is more, Alg will undergo over swelling or even degradation at excessively high temperature leading to increased leakage of ions and ligands, thus resulting in the newborn MOFs crystallization in the solution due to reduced entanglement [23,54]. Therefore, the selected reaction temperature should be able to balance the above relationship.

2.1.3.3. *Solvents* Solvents regulate the nucleation process of MOFs by affecting the release of fixed metal ions and the movement of SA chains. Foreign organic ligands are required to compete with SA chains for metal ions so as to form crystals. Unfortunately, in aquatic environments, the affinity between Co^{2+} and SA chains was stronger than that of 2-Ml, preventing the migration of Co^{2+}. However, the addition of sodium formate could provide excess Na^+ to replace the chelated Co^{2+}, promoting the formation of ZIF-67 crystals [55]. Besides, compared with alcohol, the composite gel obtained with water as solvent was sticky and uneven in color, suggesting that the polymer crosslinking and MOF distribution were uneven [42]. This might be related to the fact that H_2O caused the SA chain to move, while methanol could freeze the SA chain, providing a stable environment for the growth of MOF nuclei [55]. Therefore, ZIF-67 generated in-situ in methanol solution exhibited a better dodecahedral structure and smooth surface.

2.1.3.4. *Additives* In the synthesis process of MOFs without templates, the addition of appropriate additives can regulate crystal formation by affecting the coordination between metal ions and organic ligands. Moreover, most of them control crystal size and morphology by adding co-modulators, capped ligands, and other molecules to the synthetic medium [56]. The former refers to molecules with similar chemical structures or carrying functional groups with the same coordination ability compared to ligands, while the latter represents long-chain ligand molecules such as hexadecyltrimethylammonium bromide. In contrast, it may be because SA itself helps to control the crystal size of MOFs, and there are few additional additives added in the in-situ generation of MOFs using SA as templates. However, $NaHCO_3$ had been shown to help in ZIF-67@Alg obtaining large mesopores and high pore volume during in-situ formation process [57]. In addition, adding some modulators that can

sensitize organic ligands may be advantageous. For example, triethylamine can reduce the crystallization nucleation time by accelerating the deprotonation of carboxylic acid organic ligands, in order to obtain smaller UiO-66 crystals [58]. On the contrary, the higher the concentration of regulator acetic acid, the lower the degree of deprotonation of carboxyl ligands, resulting in a decrease in crystal nucleation and growth rate, leading to the formation of larger MIL crystals [59].

2.1.3.5. *pH* The strength of coordination bonds determines the thermodynamic stability of MOFs, and the Pearson hard acid and soft acid and base principle can be used to predict coordination strength [60,61]. Generally speaking, the combination of hard bases (such as carboxylic acid ligands) with high valence metal ions, and soft bases (such as imidazole salt ligands) with soft divalent metal ions is expected to form stable crystal structures. Furthermore, pH value is an important factor affecting the stability of MOFs, and the influence of pH on different MOF crystals is heterogeneous [62]. In acidic environments, it is mainly the coordination competition between protons and metal ions with organic ligands that hinders the formation of MOFs. In alkaline environments, the main driving force for MOF decomposition is the substitution of organic ligands with hydroxide ions. Therefore, MOFs based on high valence metal ions and carboxylate ligands are expected to be quite stable in acids, but have poor tolerance to bases. On the other hand, MOFs based on soft divalent metal ions and imidazole ligands are expected to be more stable in alkaline solutions, while they are relatively unstable in acids. That is to say, the presence of protons is detrimental to the stability of such MOF crystals. This is also the reason why most of these crystals, such as ZIF-67, are chosen for synthesis in alcohol solutions. Interestingly, the addition of additional weakly alkaline polymers such as carboxymethyl cellulose sodium facilitates the in-situ formation of ZIF-8 and ZIF-67 [63].

In summary, the in-situ generation of MOFs is influenced by various factors such as cation species, valence states, concentration, reaction time, temperature, solvents, additives, pH et al. and involves some complex microscopic mechanisms. From the perspective of cations, mainly because they have different coordination affinity, coordination number, and crosslinking mode with SA chain and organic ligands, resulting in different available nucleation sites, limited degree of crystal nucleus growth, and pore distribution of the final composite gel. In addition, on the one hand, higher temperature can improve the nucleation rate by increasing the availability and migration rate of coordination molecules and ions. However, on the other hand, because the formation of highly stable MOFs and the SA chains that can generate sufficient entanglement force with them both partially depend on the appropriate temperature, the selection of temperature needs to achieve a balance between them. In addition, although SA linkages themselves contribute to the regulation of crystals size and morphology, the addition of additional capped formulations and regulators also helps to form composite structures with more ideal microscopic characteristics. Finally, the reaction system using alcohol as a solvent not only has a certain fixation effect on the SA chain, but also avoids the negative impact of protons on

MOF nucleation in the reaction medium. Because pH is an important factor in the stability of MOFs, alcohol solutions can provide a relatively stable environment, which is conducive to the formation and dispersion of nuclei.

2.2.　*Crosslinking polymerization method*

Cross linking polymerization refers to the synthesis of target crystal structure by various methods under appropriate conditions, and then blending with SA based polymer solution to prepare the ultimate composite gel through induced crosslinking or spontaneous polymerization. Among them, spontaneous polymerization refers to encapsulation achieved solely through physical interactions within SA and SA-MOF crystals, without crosslinking metal ions. Obviously, this method will result in low load of MOFs. However, this may be attractive in some cases. For example, 15% low load ZIF-8 of SA gel could form flawless film with ideal crystal dispersion, physical flexibility, and large gas adsorption area [64]. Furthermore, Shang et al. used the ice template method to obtain ZIF-8/ SA composite hydrogel, which had relatively superior networks with increasing hydrogen bonds due to the favorable low-temperature environment [65].

However, in more cases, the mixture of MOF and SA would be further immersed in ions curing solutions such as Ca^{2+} and Tb^{3+}, thus forming a dense network on its surface due to them fast crosslinking ability while retaining the ideal appearance shapes [25,66,67]. This simple impregnation method is called exogenous crosslinking method or titration molding method, accompanied by a Ca^{2+} content gradient from the outside to the inside and an un-crosslinked core [11]. Correspondingly, there is also an endogenous crosslinking method, which involves adding cationic sources such as $CaCO_3$ to the mixed system to form a relatively uniform crosslinking network with the sluggish dissolution of calcium ions. However, $CaCO_3$ solids may be retained in the gel network together with MOF, which may cause hidden dangers. To avoid that, after mixing $CaCO_3$ nanoparticles with complex solution by ultrasound for 1.5 h, the mixed system was stewed under acidic conditions induced by hydrochloric acid for 48 h to avoid the residue of solid $CaCO_3$ [68]. Compared to the in-situ synthesis method, crosslinking polymerization method inevitably leads to poor crystal polymer interactions and particle aggregation [26]. The introduced of additional multiple chemical crosslinking reactions into the SA mixing system to form IPN may be useful, which will be detailed in Section 3.1.

In addition, due to the independent synthesis steps of MOFs, the crosslinking polymerization method supports novel MOFs combinations obtained by complex multistage processes. For example, ZIF-8 was coated onto the surface of a novel metal organic ligand framework (Zn2) through liquid phase epitaxy (LPE) method [69,70]. Simply put, it was induced by alternating immersion of Zn2 into metal ions and ligand solutions to induce the self-assembly of ZIF-8 on Zn2 surface. The successful loading of two MOFs was attributed to the abundant exposed metal sites on the surface of Zn2. (Fig. 4A). Furthermore, the composite MOF is further crosslinked and mixed with SA to form a sol that can be sprayed on the surface of food and color developed for the detection and removal of pesticides. In addition, the MOF derivative magnetic

iron/porous carbon (MagFePC) formed by MIL-100 calcination at 700 °C in nitrogen environment could also formed Alg beads with Alg by titration molding method, with MagFePC mainly composed of zero valent Fe for Fenton reaction [71]. Of course, the crosslinking polymerization method is also suitable for 3D printing. Simply immerse the composite in an ion solution that could induce rapid crosslinking after printing into the desired shape [72].

By comparison, the merits and demerits of three different synthesis routes are obvious. Among them, the two in-situ generation methods are the most susceptible to external conditions, while bring superior crystal-polymer interactions as well as good crystal dispersion. However, it inevitably generates low load capacity, which barrier may be broken through selecting appropriate crosslinking ions, metal nodes, reaction conditions, and process flow. The crosslinking polymerization method provides more possibilities for composite gel, because it can easily realize the effective encapsulation with wide load range of various MOFs, including super composites. However, the interaction force is weak and the crystals are easy to gather, thereby possibly requiring the assistance of additional dispersion strategies. In addition, the composite gel obtained from different reaction systems have different characteristics, which are closely related to the growth of crystal nuclei and the microstructure of gel. Some relevant contents are summarized in Table 2.

3.　The micro-fabrication strategy of MOF@Alg

3.1.　*Application of IPN*

The introduction of secondary network structure helps improve the physicochemical properties and performance of composite gel by changing the crystal dispersion, load, crosslinking degree, and mode, etc. The first thing worth mentioning was the introduction of chitosan (CS), which can effectively increase the porosity of the composite gel compared with the pure Alg carrier [30,82]. Furthermore, CS could be modified by quaternary ammonium salt and used in composite gel, which endowed gel with the ability to capture and kill bacteria due to the increased surface positive charges and quaternary ammonium groups [83,84]. However, when using CS-rich polymer as a template to in-situ synthesize MOF@Alg by two step method, attention should be paid to the addition order of ligands and the amount of CS. Because although the -NH_2 group on CS helped to enhance the interaction between gel and MOF crystals such as HKUST-1, ZIF-8, etc., it also prevented the self-assembly of metal ions and ligands due to the donation interaction ($NH_2{\rightarrow}M$) [23,85,86]. Therefore, excessive CS was not conducive to the generation of MOF, while adding CS after crystal assembly seemed more reasonable. PVA, a biocompatible synthetic polymer, was proved able to effectively deposit and form a protective layer on the surface of MOFs [87,88]. Especially, after low temperature freezing treatment, PVA could form a large number of hydrogen bonds forming a soft topological structure, which might provide the loss modulus to improve the tensile properties of composite gel (Fig. 5A) [36]. What is more, it supported the generation of multiple MOFs while
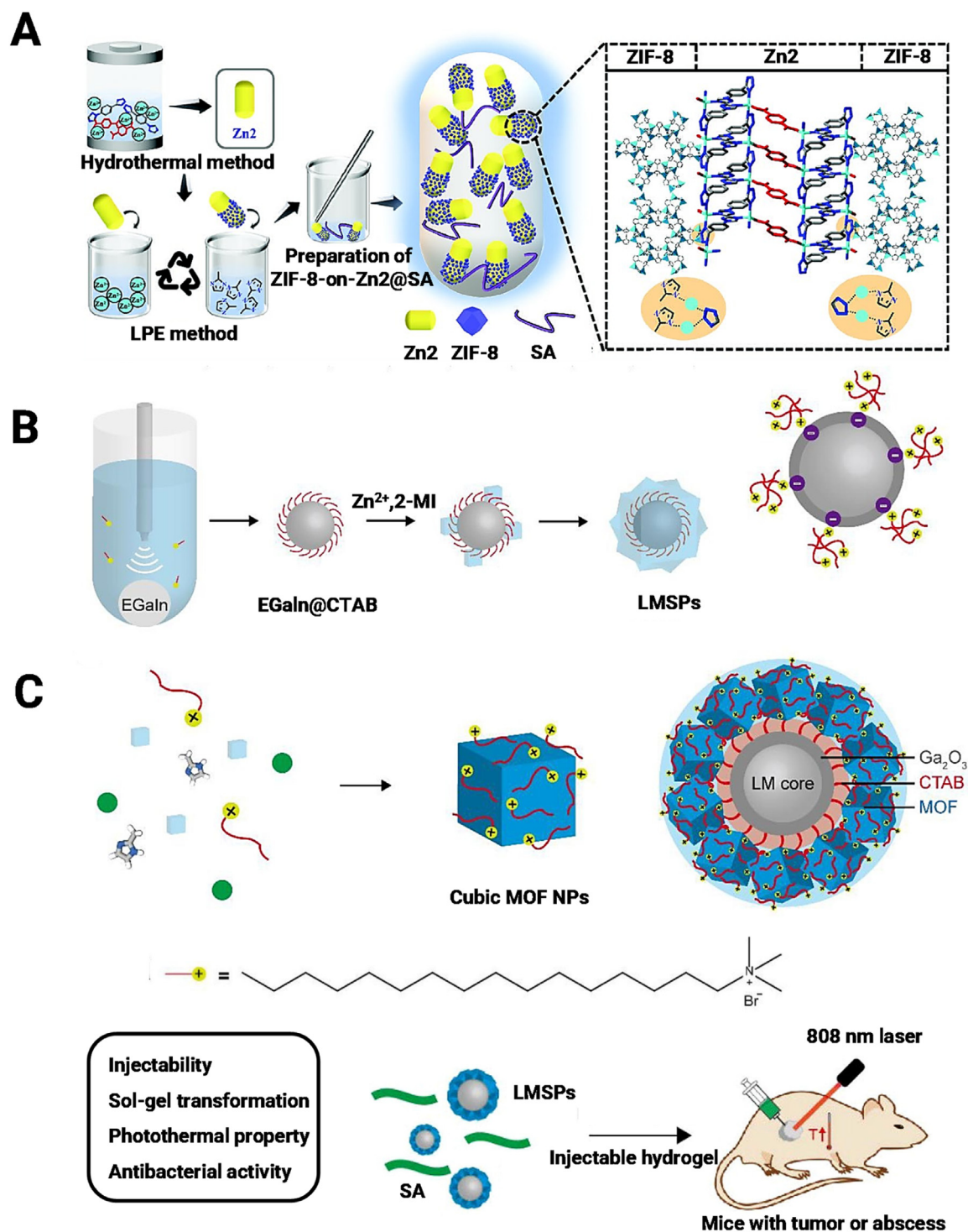
Fig. 4 – (A) The LPE method synthesis procedures and molecular microstructure of ZIF-8-on-Zn2. Reproduced from [69] with permission from Wiley. (B) The process of in-situ generation of ZIF-8 crystals on liquid gallium (EGaIn) surface mediated by hexadecyltrimethylammonium bromide (CTAB) to obtain core shell super particles (LMSP). Reproduced from [20] with permission from Elsevier. (C) Schematic diagram of CTAB as the linker and ZIF-8 surface modifier. Reproduced from [20] with permission from Elsevier.

Table 2 – Nucleation and pore characteristics of composite gel through different manufacturing methods and metal nodes.

Nucleation ion	Crosslinked ion	Interaction site with Alg	Ligand	Manufacturing method	Nucleation and pore characteristics of gel	Ref.
Cu^{2+}	Cu^{2+}	G-, M-, MG-, no priority selection	BTC	Ligand diffusion in situ generation	The outer surface formed a small-sized Cu-MOF-Alg semi crystalline structure with a wrinkled and dense microstructure.	[36,40,73,74]
				Ion diffusion in-situ generation	The outer surface had small and dense crystal nuclei, while the inner crystal nuclei were large and loosely distributed.	[40,41]
			N_2PMP	Ligand diffusion in-situ generation	The Cu^{2+} was partially reduced, resulting in crystal nuclei growth uneven.	[39]
	Ca^{2+}	G-, MG-, G- is main	AZPY	Crosslinking polymerization	Forming standard HKUST-1 crystals with uniform distribution, but the crystals were covered by Alg.	[75]
Zr^{4+}	Cu^{2+}	Ditto	H_4btec	Crosslinking polymerization	The crystal nucleus agglomerated to a certain extent, and many irregular micropores in the gel.	[76]
	Ca^{2+}	Ditto		Electrospinning technology and crosslinking polymerization	The MOFs loading was 16 wt%, with some degree of aggregation of crystal nuclei and relatively loose epidermal layer.	[43]
Co^{2+}	Co^{2+}		2-MI	Electrospinning technology and ligand diffusion in-situ generation	The ZIF-67 with clear and regular crystal structure grew on the surface of fibers.	[32]
				Ligand diffusion *in situ* generation	The low Co loading (2.00 wt%) and the gel surface was relatively smooth with pore of 2.5~12.5 nm.	[42,63]
				One-step generation	The MOF-like structure was generated and the surface of gel was flower-like particles.	[42]
Ni^{2+}	Ca^{2+}	Ditto	2,5-DA	Crosslinking polymerization	The CPO-27-Ni crystals were tightly packed, and pore free gel was formed between aggregates.	[77]
Zn^{2+}	Ca^{2+}, Zn^{2+}	G-,MG-, mainly G- (Zn^{2+} is single tooth mode and Ca^{2+} is double tooth one)	2-MI	Ion diffusion in-situ generation	The ZIF-8 particles were uniformly embedded on the surface in a monodisperse form, presenting a graded porous structure, with a loading capacity of 29.33%.	[26]
	Zn^{2+}			One-step in-situ ball milling method	The ZIF-8 had a good crystal structure and exhibited a certain degree of aggregation.	[31]
	Ca^{2+}			Crosslinking polymerization /PVA	Successfully encapsulated tyrosinase.	[78]
	Eu^{3+}		Bpbenz and H_3BTC	Crosslinking polymerization	The layered Zn-MOF was well dispersed in the gel network forming a good dry film material.	[79]
Fe^{3+}	Ca^{2+}	Ditto	H_4ABTC	Crosslinking polymerization/ PAA	The MIL-127 was evenly distributed in gels with an ultra-high loading capacity of over 90% and superior stability in aqueous solutions for several months.	[80]
	Fe^{3+}	G-,M-,MG-	H_3BTC	Ligand diffusion *in situ* generation	The MIL-100 growth was strictly restricted and distributed dispersedly, with dense polymer walls and continuous presence of many ice-crystal like cavities.	[51,36,53]
Ti^{4+}/Fe^{3+}	Ca^{2+}	Ditto	BDC	Crosslinking polymerization/ CNT	Forming regular spherical microspheres without cracks.	[15]
Al^{3+}	Ca^{2+}	Ditto	H_4BTC	Crosslinking polymerization	The load capacity of MIL-125 was up to 50 wt%.	[81]

Abbreviation: 2,5-Dihydroxyterephthalic acid (2,5-DA); 1,4-bis(pyrid-4-yl)benzene (Bpbenz); 3,3′,5,5′–Azo-benzene tetra carboxylate (H4ABTC); 1,4-Benzene dicarboxylic acid (BDC); Homo-mellitic acid ligand (H4BTC); polyvinyl alcohol (PVA); polyacrylic acid (PAA); carbon nanotube (CNT).

Fig. 5 – (A) The process of PVA and SA crosslinked by freezing and ion curing and in-situ induced growth of MOFs to form composite hydrogels. Reproduced from [36] with permission from Elsevier. (B) Histograms of the interaction forces between different combinations of Ca^{2+}, PAA, and Alg (the image on the far right). The molecular microstructure of PAA/ Ca^{2+} and PAA/ Alg obtained from MD (two images on the left). Reproduced from [80] with permission from American Chemical Society. (C) The schematic diagram of grafting polymerization of methacrylic acid hyaluronic acid (HEMA) and SA (SA-GMA) with acrylic acid (AA) modified UiO-66 through solvent assisted light grafting reaction (SALI). Reproduced from [97] with permission from Elsevier Ltd.

improving mechanical properties [89-91]. Cellulose is one of the most abundant polymers, with abundant hydroxyl groups on its surface, which form strong intermolecular and intramolecular hydrogen bonds resulting in itself aggregating to form a crystal structure [92]. Zhao et al. used cellulose nanocrystals and CS/ SA as polymer templates to induce the synthesis of Cu-MOF [93]. Among them, cellulose could act as the filler of gel network and bridged SA and CS through intermolecular hydrogen bonds to obtain porous hydrogels with enhanced strength. Porous structures could promote the diffusion of metal ions, thereby increasing the MOF loading capacity.

In order to associate the newborn MOF nucleus with Alg network instead of being isolated in the solution, it was a common operation to wash the crosslinked Alg with solutions such as ethanol to remove excess metal ions before the step of nucleation [36,39]. In addition, additional crosslinking methods could also be considered to effectively intercept the new MOF core, especially for the loosely structured and fragile Alg such as Zn-Alg. That was potentially because the association mode between Zn^{2+} and SA unit was single tooth "egg-box" which was different from the double one of Ca^{2+} [94]. Lin et al. used sodium carboxymethyl cellulose (CMC–Na)/ Polyetherimide (PEI)/ Alg as the polymer carrier to anchor Zn^{2+}

for in-situ generated ZIF-8. Subsequently, the crosslinking agent epichlorohydrin (ECH) was added to initiate crosslinking between imino, carboxyl, and hydroxyl groups on the side chains of each polymer, which could effectively intercept the crystal structure while improving the mechanical strength of materials [63]. However, owing to a large amount of protonated ammonium groups contained within PEI, it could rapidly self-assemble with SA negatively charged forming even composite hydrogel, which was in favor of nucleation ions diffusion [95]. However, the existence of PEI occupied the crosslinking sites of the metal ions simultaneously, resulting in reducing mechanical strength of the composite hydrogel [74]. There was also another sample method to introduce the second crosslinking network without additional crosslinking agent. Typically, adding PAA in curing Ca^{2+} solution, PAA could crosslink with Alg and Ca^{2+} thereby introducing hydrogen bonds and ion interactions [80,96]. Of course, due to the potential of the -COOH on PAA to form hydrogen bonds and bind to metal ions on the MOF surface, composite materials also could be successfully prepared without additional ion curing steps [69]. Nevertheless, the interaction between Ca^{2+}, PAA, Alg, and MIL-127 had been investigated by molecular dynamics simulation (MD), indicating that the binding energy of Ca^{2+}/ PAA/ Alg composite was the highest compared to Ca^{2+}/PAA, Ca^{2+}/Alg, and PAA/Alg and the interaction force presented between both polymers and MIL-127 [80] (Fig. 5**B**). Additionally, the combination of PAA and Ca^{2+} could lead to the discharge of water, which might also be one of the reasons why PAA enhanced the mechanical strength of composite gel.

As mentioned earlier, hydrogels containing MOFs can be finely prepared by 3D printing. The shear thinning and rapid prototyping properties are important for biological ink. The combination of SA and acrylamide is considered an ideal printable ink with the help of shear thinning agents [41]. However, it is worth noting that since the ions of the organic ligands or other molecules in the system will shield electrostatic forces, which is the main mechanism commonly used as ion shear diluents, it is more reasonable to choose non-ionic diluents. When using gelatin as the second network to crosslink SA for 3D printing, there is no need for shear thinning agents due to the good shear thinning properties of gelatin [72].

In conclusion, compared with pure Alg, the dual network topology has great advantages in assisting MOFs crystal dispersion, enhancing crystal-polymer interactions, improving the pore size characteristics and mechanical strength of composite gel. However, when introducing certain polymers rich in amino or imino groups such as CS and PEI, some additional impacts need to be taken into account. Due to the strong donor nature of amino groups and the charged nature of protonated amino groups, while the interactions of mature MOF crystal-polymers and polymers-polymers are enhanced, these polymers may hinder the self-assembly behavior of MOFs due to the tight chelation of amino groups on nucleation ions and the occupation of carboxyl sites of SA by protonated amino groups. This can be avoided by early addition of ligands to induce nucleation. Finally, with the help of polymers or non-ionic diluents with shear thinning properties, MOF@Alg can form through 3D printing.

3.2. Modification strategies

3.2.1. Chemical modification strategies

Compared to non-covalent bonds, covalent bonds between crystals and polymer networks are more conducive to the loading of MOFs, especially for crosslinking polymerization methods. To this end, through SALI, a typical acid-base reaction, AA was successfully inserted into the crystal structure of MOF UiO-66, resulting in the presence of vinyl groups on its surface [97]. The successful modification of the MOF structure was attributed to its defective structure, which had been widely recognized [98]. Furthermore, SA was functionalized by glycidyl methacrylate and achieved the growth of graft polymer chains with initiator to induce after the modified UiO-66 was added, ultimately forming elastic hybrid hydrogel (Fig. 5**C**). Similarly, dropping N, N-dimethylformamide into the precursor solution for UiO-66 synthesis could successfully prepare UiO-66-$(NH_2)_2$ nanoparticles. The introduction of $-NH_2$ allowed for the formation of secondary chemical crosslinking networks initiated by glutaraldehyde after Ca^{2+} gelation, significantly enhancing the interaction with Alg networks and achieving effective encapsulation of MOF crystals [99]. In addition to the naturally occurring defect structures on the surface of MOFs, engineered defects can also improve the performance of crystals. The defect rich Co-MOF (CoBDC-Fc) induced by ferrocene dicarboxylic acid (Fc) had higher enzyme loading capacity and protein capture ability, which can greatly improve the catalytic efficiency of composite materials [100]. More interestingly, besides the modified microstructure of the MOFs crystal itself, the novel crystal based on MOFs such as LMSP formed by MOF chemical coating have more attractive properties. Specifically, coated liquid eutectic gallium indium nanoparticles (EGaIn) with ZIF-8 and the successful encapsulation of ZIF-8 was attributed to the addition of the inter particle linker CTAB (Fig. 4**B**) [20]. Among them, the cationic head of CTAB undergone electrostatic binding with the oxidized EGaIn surface, while the free CTAB entangled ZIF-8 to regulate its size. Finally, the two particles formed LMSP through self-assembly (Fig. 4**C**). Furthermore, LMSP was bound to gel network due to electrostatic interaction between Zn^{2+} of defect MOF and carboxyl groups of SA and formed viscoelastic gel for tumor treatment under physiological conditions after being injected into the body.

As is well known, the pores of MOF largely determine its function. In order to obtain controllable UiO-66 with different graded pores, Yang et al. pre-doped the unstable semi-ligand 2-nitroterephthalic acid in the crystals structure and crosslinked them with Alg to obtain composite with expanded pore particles for effective adsorption of bisphenol A [101]. Besides MOFs modification, porous graphite carbon (PGC) derived from natural materials such as Alg and cellulose had high porosity and large surface area. Meanwhile, PGC supported the in-situ generation of MOF crystals such as MIL-88B, but the morphology of the final composite strongly depended on the amount of PGC added. Compared with other additions, 50% PGC addition could cause partial collapse of the MIL-88B crystal structure, which was unfavorable for both molecular adsorption and drug loading [102].

3.2.2. *Physical modification strategies*

Physical modification refers to the mixing of some functional materials such as graphenoxide nanosheets (GO), modified GO, Mxene, CNT, etc. with SA through simple physical interactions to improve the network crosslinking of gel or the dispersion of MOF crystals. Usually, owing to the characteristic groups on the surface of these materials, they all contribute to the dispersion of MOF crystals to some extent. For example, the addition of GO in soluble Alg solution was in favor of anchoring cation ions better [33,37]. It could interact with Alg chain through strong hydrogen bonds while binding to Co^{2+}, which thus were bound in novel "egg-box" like models with high dispersibility [37,57]. In contrast, the crosslinking between Co^{2+} and pure Alg chains was uneven, resulting in random growth of MOFs. Furthermore, GO modified by carboxyl group (GOCOOH) could further enhance the interaction with Alg, which was attributed to effectively improve the mechanical strength of composite gel thus preventing cracks after drying [103]. Meanwhile, carboxyl and other oxygen-containing groups of GO as well as reduced graphene oxide (rGO) provided more action sites, which was advantageous [103,104]. Similarly, the addition of an appropriate amount of CNT could also improve MOF dispersion [15]. Interestingly, the enhanced hydrophobicity from CNT might support an ideal platform for loading and adsorption of hydrophobic drugs and organic molecules. Mxene, a synthesized two-dimensional ultra-thin ceramic nanosheet, could physically combine with MOF to produce stable and porous sandwich like composite nanostructures with high surface area and extraordinary stability similar to GO/MOF composite [30]. Of course, under harsh hydrothermal synthesis conditions, Mxene with negative surface charges also supported in-situ generation and uniform dispersion of positively charged MOFs through multiple physicochemical interactions by massive -OH and -COOH groups of the Mxene [105].

3.2.3. *Targeted modification strategies*

Although the encapsulation of SA can protect MOFs to a certain extent and improve biocompatibility, controlling the interaction of particle interfaces in the biological environment is still necessary for drug delivery systems due to the influence of the circulatory system [106,107]. Fortunately, delicate and effective targeted modification can improve the bioavailability of MOF composite particles to some extent. It is advantageous to pre-coat MOF particles with ligand proteins on their surface, which will not only endow them with targeting properties but also help to reduce unexpected interface interactions with non-target substances. Specifically, Zr_6-MOF (PCN-224) was coated with a targeted affinity ligand protein fused with glutathione transferase (GST-Afb) through simple mixed coupling [106]. Among them, GST adsorbed on the porous surface, and the Afb connected by GST formed outward, which could minimize the interface interaction between particles and external biological proteins. Due to the presence of unsaturated sites on the surface of MOF crystals, they are easily occupied by carboxylic acid groups in proteins or phosphate groups in DNA, leading to protein corona phenomenon and further clearance by macrophages easily [108]. However, the modified PCN-224 can effectively shield protein corona phenomenon while being accumulated at the tumor site leveraging the ability to target cells of Afb. Besides, biofilm modification is considered an effective strategy in helping nanoparticles achieve immune system escape and targeted accumulation [109,110]. For example, in order to track infiltrating glioblastoma multiform (GBM) cells and tumor microsatellites, Zhang et al. extracted glioma associated macrophage membranes (GAMM) from glioma bearing mice. Because the vascular cell adhesion molecule-1 expressed by brain tumor cells and the integrin axis $\alpha 4\beta 1$ on the surface of macrophages driven tumor migration made them the most abundant cell type in the GBM microenvironment [106]. Subsequently, mitoxantrone and the small interfering RNA targeting indoleamine 2,3-dioxygenase-1 were loaded in ZIF-8 particles and further co-extruded with GAMM through polycarbonate porous membranes to obtain the GAMM-modified core-shell composite structure [111]. After the composite system was further loaded into the hydrogel and delivered to the resected tumor cavity, it would imitate the "hot" tumor immune niche, achieving continuous T cell infiltration, to attack the remaining tumor cells and significantly inhibit the recurrence of GBM after surgery.

In brief, both the SA-based polymer matrixes and the loaded MOF crystals can be physically or chemically modified to achieve enhanced ideal performance. Physical modification mainly refers to the addition of 2D materials with special functions, which can serve as excellent connectors or platforms to improve the dispersion of MOF crystals while enhancing particle-polymer interactions. What is more, they are potentially in favor of supporting the loading and adsorption of more types of molecules. Chemical modification refers to the large-scale modification of the matrix under extreme conditions or the partial modification of functional groups through certain chemical means, both aimed at enhancing the interaction forces between phases or obtaining the required structural characteristics such as high porosity. Furthermore, targeted modifications can be applied to the surface of MOFs through physical or chemical means to enhance their bioavailability or the drugs they carry. In addition, it seems to be an interesting and promising way to obtain new composite gel materials with additional properties by assembling on traditional MOFs through certain technical means.

4. Macroscopic application forms and advantages of MOF@Alg

4.1. *Composite beads and fibers*

Typically, Alg composite beads are formed by selectively dropping a mixed solution containing MOF into curing solution richen metal ions and if being continuously injected will obtain composite fibers [112,113]. Calcium chloride solution is the most commonly used molding solution, and it has been proven that a concentration of 2%–3% (w/v) can induce suitable bead formation kinetics thereby forming perfect MOF containing spherical beads in about 10 min. And longer gelation time will not cause a significant increase in mechanical strength [9]. The success of spherical beads is

largely due to the standard double tooth "egg-box" model followed when Ca^{2+} is crosslinked with Alg, which helps to form a uniform and dense gel network. In contrast, Zn^{2+} and Fe^{2+} are rarely used alone for the curing of composite beads because the networks crosslinked by them is loose and fragile (Fig. 7A) [94]. This is also in line with the viewpoint in existing research that different solidified cations produce diverse shaped beads [9]. Among them, in order to obtain ideal spherical beads of Al^{3+} and Zr^{4+}, the mixed liquid required to pre-cure in Ca^{2+} solution and subsequently transferred to Al^{3+} or Zr^{4+} gel bath for 90 min [9]. By contrast, Cu^{2+} allowed the formation of dense and thick cementitious layers, increased the mechanical strength of beads, and inhibited the shrinkage of gel, so it was often used for the crosslinking nodes of composite gel beads, which could be shaped under a lower concentration (about 1.3%, w/v) [11,76]. In addition, the strength of Alg-Cu beads prepared under the same conditions was significantly weaker than that of Alg-Ca beads, which might be due to the rapid gel induced by the high affinity between Cu^{2+} and Alg, resulting in the thickness of the outer insoluble scaffold being thinner than that of calcium alginate [9,11].

The biggest advantage of Alg beads lies in their high stability, excellent mechanical strength, tunable particle size, and easy preparation and recycling. Therefore, Alg particles can effectively resist gastrointestinal peristalsis and the damage of acidic environments to the payload [114]. Ideally, if the size is appropriate, Alg beads can penetrate the colonic mucosal layer for effective siRNA delivery. Among them, due to the dispersion of Alg and MOF structures throughout the beads, the insoluble Alg in the outer layer serves as a 3D framework to withstand external pressure (Fig. 6A). Therefore, as the content increases, the strength of the beads will also increase. However, for the crosslinking polymerization method, excessive Alg concentration (usually slightly higher than 2.0%, w/v) is not conducive to the uniform distribution of MOF crystals due to the increase in solution viscosity [9].

4.2. Composite film

Compared with hydrogel beads, gel films have attracted more and more attention due to their extraordinary mass transfer performance and flexibility [115]. The good plasticity of Alg endows it with film forming characteristics. However, most pure polysaccharide films lack mechanical strength and have relatively poor selectivity [92]. Incorporating porous crystalline MOFs fillers into the Alg membranes can increase their relative surface area while enhancing the mechanical stability of the composite membrane. The former is attributed to the high pore properties of MOF materials, which also endows hybrid membranes with high selectivity. The latter is due to the chemical or physical interactions between the metal centers or organic ligands of MOFs and the carboxyl and hydroxyl groups of Alg [92,116]. It is worth noting that obtaining a highly stable homogeneous sol with a certain concentration is the primary condition for preparing a crack free and uniformly structured film. For the Alg-MOFs sol system, larger molecular weight SA and agglomerated MOFs nanomaterials are not conducive to film formation, resulting in membrane cracking and uneven structure. Therefore, it

is important to mix MOFs and Alg solution evenly before curing. Hence, in addition to conventional stirring treatment for the mixed solution, using a sand core filter to remove agglomerated polymers or MOFs particles under a certain pressure is proved a good choice [115]. On the other hand, suitable synthesis strategies are also important for ideal composite membranes. As mentioned earlier, due to the poor dispersion occurred more likely during one-step synthesis processing, another two methods were more applicated in membrane fabrication. Furthermore, PVA rich in -OH was introduced into the SA network to participate jointly in chelating with metal ions, so as to subsequently initiate *in situ* MOF generation. Among them, PVA increased the adhesion of gel films while providing more uniform nucleation sites to prevent the film from falling off [14].

In addition to the conventional coated hydrogel films, SA also supports the construction of fiber gel films, which can be used as fiber material or substrate material. Specifically, polyacrylamides (PAM) was used together with SA as a substrate for electrospinning to form a gel network with 3D spatial structure, which acted as the polymer template to induce self-assembly of ZIF-67 after solidification with Co^{2+} [32]. It may be attributed to the more ordered and controllable network structure. The ZIF-67 crystal generated in-situ better retains the crystal structure and reduces the entanglement with the gel chains (Fig. 7B). The resulting graded porous structure may be advantageous. In contrast, fibers formed by blending polymer solutions before electrospinning do not exhibit obvious crystal contours [43]. As the amount of MOF added increases, fibers exhibit nodular structures due to crystal aggregation (Fig. 7B). As a result, many voids have been formed along the nanofibers, which are believed to facilitate the entry of solutions [117].

4.3. Aerogel and cryogel

The Alg-based aerogel and cryogel have been used in tissue engineering, drug delivery due to the special properties [118-120]. However, the concepts of aerogel and cryogel are always confused. In fact, the term aerogel is related to the samples of aqua-gel dried using supercritical carbon dioxide [121]. The benefit of using this process is to obtain aerogel having small pores [122]. Nevertheless, The Products commonly obtained only through freeze-drying procedures in literature are cryogel, which have huge holes [123]. Compared with other forms, the mesopores formed by freeze-drying and micropores formed by MOF make the composite gel a 3D material with hierarchical porous structure, high specific surface area, and low density [124]. In addition, compared with the traditional freeze-drying procedure, the directional freezing method supports the directional growth of ice crystals along the temperature gradient. As a result, the regular pore structure will be formed after sublimation and the pores inside the gel will be prevented from collapsing due to inner capillary pressure simultaneously [65]. Specifically, it was to replace the traditional freezing treatment with a gradient cooling ice template freezing method. During this process, MOF particles would be arranged or embedded with the directional growth of ice crystals, and uniformly deposited on the Alg pore wall after drying, which were conducive to
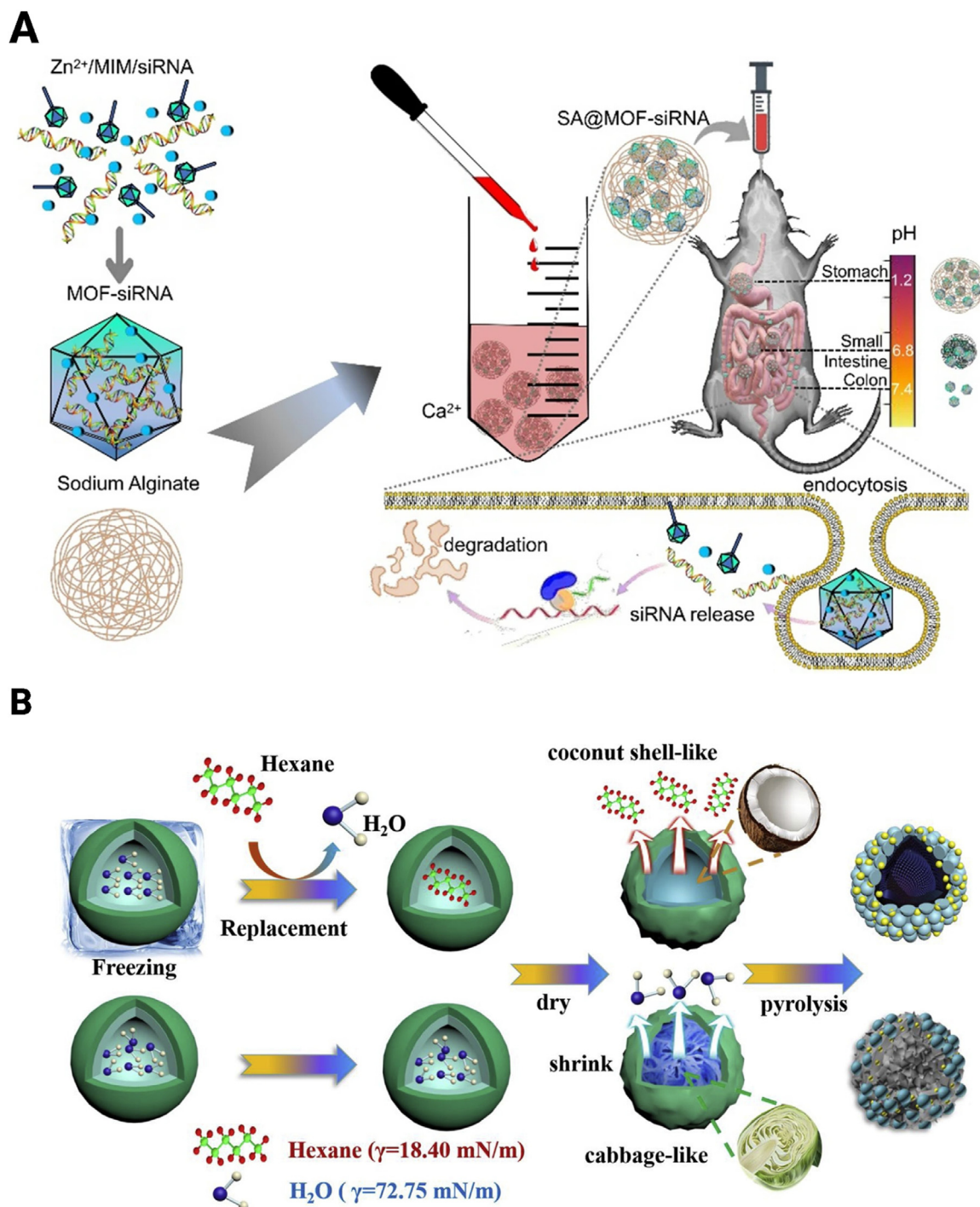
Fig. 6 – (A) Schematic illustration of the proposed SA@MOF-siRNA for the treatment of ulcerative colitis. Reproduced from [114] with permission from BioMed Central. (B) MOFs coated hollow structured carbon composites formed by replacing solvents of H$_2$O with hexane or not, exhibiting microscopic morphological differences. Reproduced from [38] with permission from Elsevier.

the full exposure of MOF particles (Fig. 7C). Furthermore, the corresponding carbon aerogel could be obtained by calcining and activating the aerogel at a certain high temperature N$_2$ [65,125]. After that, the 3D gel skeleton and many oxygen-containing functional groups were still retained, but the partial collapse of Alg and MOF condensation could form

micropores, which was conducive to the exposure of active sites. Moreover, the Raman and Pore VSM analysis showed that the formation of defect structures was related to the type of metal ions. Compared to Cu, using Fe as a metal ion node was more likely to induce the formation of defect structures during the carbonization process [125].
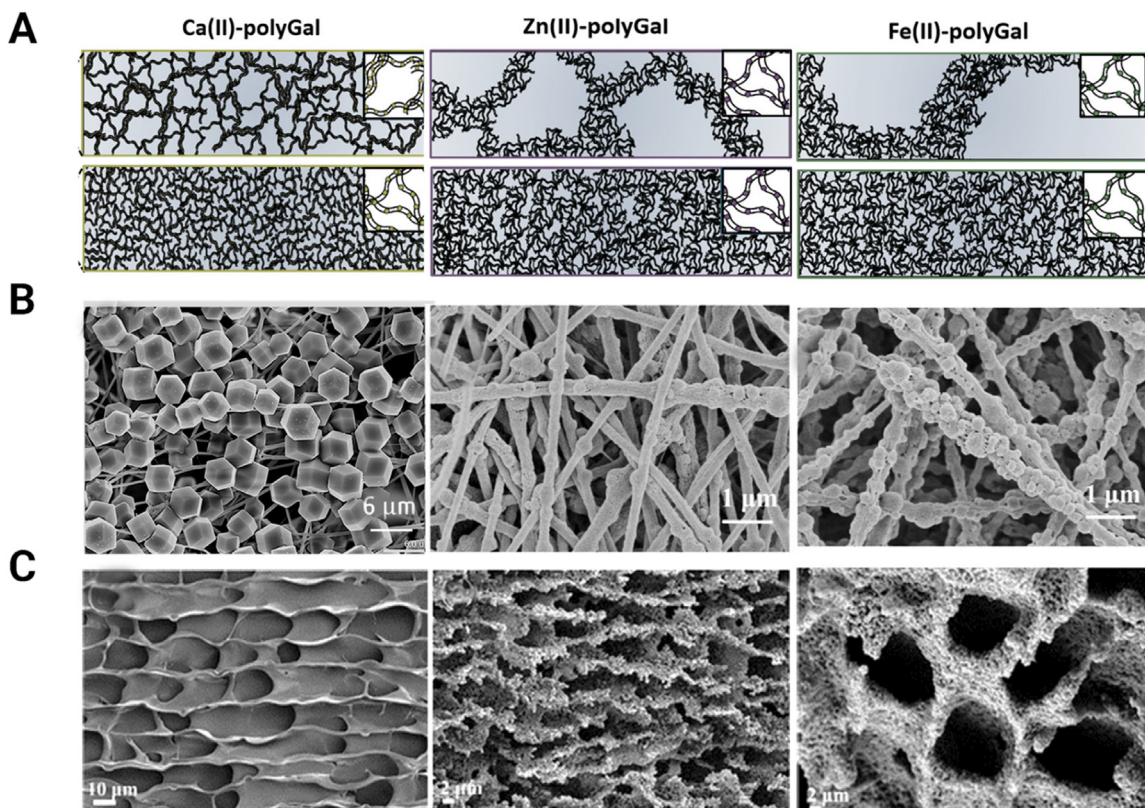
Fig. 7 – (A) The schematic diagram of crosslinking modes between Ca^{2+}, Zn^{2+} and Fe^{2+} with SA. Reproduced from [94] with permission from American Chemical Society. **(B)** The microstructures of MOF@Alg fiber membrane obtained by electrospinning followed by in-situ generation (far left figure) and in-situ generation followed by electrospinning (the two figures on the right represent low and high loading, respectively). Reproduced from [43] with permission from Elsevier. **(C)** From left to right are the microstructures of original SA formed by directional freeze-drying, ZIF-8@Alg hydrogels, and ZIF-8@Alg carbon aerogels. Reproduced from [65] with permission from American Chemical Society.

4.4. Other forms

In addition to the three common forms mentioned above, the flexibility of SA supports the formation of multiple composite gels with customized structures. Firstly, owing to in-situ deposition of MOF crystals with the help of SA, defect free MOFs coated hollow structured carbon composites, with large surface area and excellent electronic conductivity, can be successfully assembled and produced on a large scale [38]. The hollow carbon wall of the composite material was formed by SA pyrolysis. Specifically, SA spheres were solidified in a 20 wt% $CuSO_4$ solution and used for Cu-MOF coating under suitable conditions. After sequential freeze-drying, vapor deposition of Fe_3O_4, and SA pyrolysis, bimetallic hollow carbon composites were obtained. Thereinto, the high concentration of Cu^{2+} solution might be the reason why the MOF core mainly grew on the surface of the gel ball rather than inside. In addition, the traditional hot drying strategy was replaced by the freezing substitution strategy (F-R) in this experiment. Water with high surface tension was substituted by hexane with low surface tension, subsequently being removed during the drying process to form the inner wall of the hollow structure with low shrinkage, thus forming a structurally stable, complete, and smooth coconut shell structure (Fig. 6B). This structure allowed active sites homogeneously distributed on no-defect surface and improved magnetic and photocatalytic activity of composites.

In addition, with the help of tubular mold, the composite hydrogel could also be coated on the surface of carbon fiber bundles to form coaxial monolithic parts with excellent mechanical robustness [126]. Interestingly, the ion concentration gradient caused by the in-situ formation of MOF could also induce the formation of tubular gel [55]. Due to the rapid released of chelated Co^{2+} from sodium formate for nucleation, a mixed aqueous solution containing 2-Ml could quickly induce the formation of a hard MOF containing Alg shell. However, due to the lack of crosslinking sites caused by the external migration of Co^{2+} inside, the loose inner core would absorb water and expand, thereby forming a tubular geometry. Finally, the printability of this composite material had been mentioned before. Composite gel with different patterns such as square, hexagon or various biomimetic shapes were available and were considered to have better recyclability [72].

Overall, relying on different operating procedures, MOFs@Alg can be shaped for different traditional forms of bead, fiber, membrane composite gel or aerogel. Because of its flexibility and stability, the bead shaped composite Alg
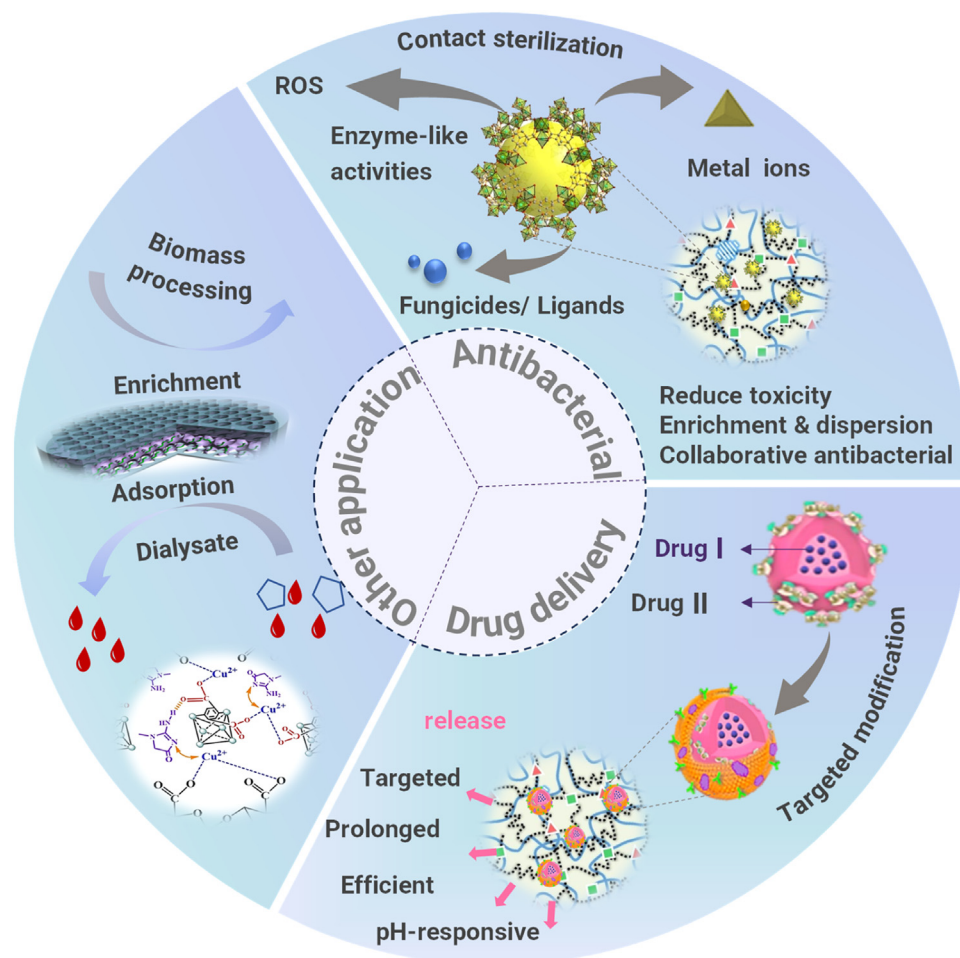
Fig. 8 – Summary diagram of MOFs@Alg biomedical applications.

gel with controllable particle size is very suitable for delivery carriers or excellent adsorbents. However, the selection of curing ions and concentration control are important. Ions such as Zn^{2+}, Al^{3+} and Zr^{4+} that have poor affinity with the SA chain will only form a loose and fragile crosslinking network with poor formability and low stability, thereby being not suitable as curing ions alone. For membranous gel, suitable MOFs loading and uniform precursor solution are significant conditions for the formation of intact and crack free gel membranes. Besides, the cryogels obtained by freeze-drying can improve the microscopic characteristics by using the qualitative freezing method. Finally, after further reasonable design, MOFs@Alg can also be manufactured into various ideal forms to meet diverse application requirements.

5. Biomedical applications

Based on high biocompatibility, low toxicity, simple gel mechanism, easy functionalization of SA, and MOF's unique structure of high loading, controlled release capability, and flexible construction form, MOFs@Alg has great prospects in antibacterial, targeted delivery, wound healing, and other aspects [112,127,128] (Fig. 8).

5.1. Antibacterial and wound healing

Researches have consistently shown that the metal nodes and organic linkers of MOFs themselves, enzyme-like activities producing reactive oxygen species (ROS), the metal ions released by the MOF frameworks, or biocidal agents encapsulated in MOF pores all can as active mechanisms destroy bacterial cell membranes and cause bacterial inactivation [129,130]. This antibacterial mechanism mainly relies on the free movement of antibacterial components in the complex wound solution environment, and then contacts and kills bacteria. However, some antibacterial substances such as ROS have a short lifespan and limited diffusion distance, coupled with the interference of the movement of bacteria, which leads to a significant decrease in the contact efficiency between bacteria and antibacterial substances, thereby greatly weakening the antibacterial effect of MOF [131,132]. The hydrogel-based composite systems can be highly suitable for various requirements in the dynamic wound healing process to promote wound healing.

Quan et al. successfully prepared Cu-MOFs using 4,4′-azopyridine ligands and loaded glutaric acid (Glu) during the synthesis process of MOFs, which was demonstrated to have excellent antibacterial effects against various bacteria

and fungi such as Escherichia coli and Candida albicans [75]. Furthermore, Cu-MOF was encapsulated in IPN formed by methacryloylated SA (MASA) so as to avoid the cytotoxicity of high dose MOF. However, the release of Cu^{2+} after crystal degradation could induce crosslinking of Alg chains, thereby hindering further ion release. Although this might partially affect its bactericidal effect, the safety hazards caused by high concentrations of Cu^{2+} could be avoided to some extent. On the other hand, the formation of the second crosslinking network also contributed to the stability of the encapsulated functional substance. For example, attributing to the secondary network formed by the release of Zn^{2+}, the liquid EGaIn coated with ZIF-8 mentioned above could better maintain the spherical structure of gallium (Ga) under multiple NIR irradiation, which was the key to the photothermal performance of composite materials [20]. What is more, Zn^{2+} was not only a broad-spectrum antibacterial agent, but also had also been proven to play an important role in various biological activities as well could promote nerve regeneration [133]. Due to the superior photothermal activity of Ga, the temperature of the composite hydrogel increased by 31 °C after 10 min of laser irradiation. Combined with the antibacterial properties of ZIF-8, the composite hydrogel showed exciting antibacterial and anti-tumor dual functions. It is worth mentioning that even in the absence of additional photothermal materials, certain metal ions such as iron, manganese, and copper ions can generate satisfactory photothermal effects when coordinated with organic molecules [134,135].

For medical bio-MOFs, in addition to selecting low toxicity metal nodes, it is meaningful to use drug molecules as organic ligands to initiate self-assemble [136]. Curcumin, a polyphenolic substance with anti-inflammatory effects, could act as a biological ligand to coordinate self-assembly with Zn^{2+} and created a favorable microenvironment for wound healing after release (Fig. 9**D**) [137]. In addition, different from the photothermal materials used to kill tumors, the composite gel containing MOFs could generate mild thermal stimulation under NIR irradiation to promote angiogenesis and avoid scalding surrounding tissues (Fig. 9**D**) [138,139]. Furthermore, positively charged quaternary ammonium CS (QCS) was integrated with Zn-MOFs preferably captured negatively charged bacteria and further damaged bacterial membranes [83]. In order to make the gel better fit the dynamic wound, methacryloyl functionalized oxidized SA (OSAMA) and hyaluronic acid were used to construct and IPN hydrogel Zn-MOF loaded, thus forming a dressing that integrated highly effective antibacterial, anti-inflammatory, neural and vascular regeneration for wound cascade repair (Fig. 9). At the same time, because of the combination of $-NH_4^+$ of CS and $-COO^-$ of SA, the crosslinking degree of gel network was reduced, thus improving the swelling ratio, which could provide a mild and moist favorable environment for tissue regeneration during a long time. In addition to Zn^{2+}, Ag^+ was also considered an excellent antibacterial agent. For this, 3,5-dicarboxylic acid pyridine was used to form a linear MOF with organic linkers and Ag^+, which was filled with CS nanoparticles in the upper layer of wound dressings, while exerting high antibacterial properties and avoiding direct contact with the skin [128]. The lower layer was composed of a biocompatible SA-rich crosslinked network, which had a uniform pore structure and good water retention ability, providing a favorable moist environment for wound repair.

Ideally, based on the designability of gel network and MOF, the composite gel treatment platform with synergistic effect seems more high-efficiency. The multifunctional dressings that meet the needs of different wound stages can exert synergistic effects throughout the whole-process healing. The dodecyl tails connected to the hydrogel could act as "spider webs" on the cell membrane through hydrophobic interaction, thus introducing the bacterial anchoring function, hemostatic performance and skin adhesion function network [140]. Subsequently, Cu-MOFs with oxidase-like activity could act as "spider teeth" to destroy the bacterial outer membrane. After the cell membrane was destroyed by MOF, the sustained-release singlet oxygen ($^1O_2$) and Cu^{2+} of the former could smoothly enter the bacterial intracellular environment in the form of "spider fluids" to kill bacteria (Fig. 10**A**). This sequential process was the reason for the highly effective bactericidal ability of the composite gel. Furthermore, reduced polydopamine nanoparticles (rPDA NPs) with phenolic hydroxyl and protonated amino groups were introduced into the hydrogel system to correct excessive oxygen free radicals that hindered the production of granulation tissue in the later stage of wound healing (Fig. 10**B**), cleverly achieving dual functions of anti-infection treatment and promoting wound healing to adapt to the dynamic wound healing process [141,142].

5.2. Drug delivery

Different from being used for antibacterial and wound repair, when MOFs containing composite gel is used for drug delivery, more consideration should be given to drug encapsulation efficiency and targeted release capacity. Besides, for MOFs, the selection of metal nodes and organic ligands has become more demanding. The endogenous metal elements rich in the human body, such as Cu, Zn, Fe, Mg, and organic ligands that can be cleared or metabolized, are optional [83]. Generally speaking, integrating with the presence of metal ions and organic ligands, porous MOFs support the enrichment of multiple drugs, between which can form electrostatic, π - π stacking, and other interactions. More excellent interaction forces and the encapsulation of biopolymers are undoubtedly beneficial for the effective loading and long-term release of drugs. For example, sheet-like Cu-MOF synthesized with non-toxic aspartic acid (Asp) as organic linker and Cu^{2+} as metal node could achieve effective encapsulation of diclofenac sodium, with a loading rate of 53.07%, which was much higher than other reported carriers [27]. Relatively speaking, due to the excellent relative affinity between metformin and the Lewis acid side of the inner surface of ZIF-8, a loading rate of 83.5% could be achieved [31]. Furthermore, drug loaded MOFs can be encapsulated into the Alg gel network to form beads, which can prevent their degradation and sudden release in the acidic environment of gastric juice and achieve sustained release in the alkaline intestinal fluid environment. Because SA chains undergo electrostatic repulsion due to deprotonation in alkaline environments, resulting in
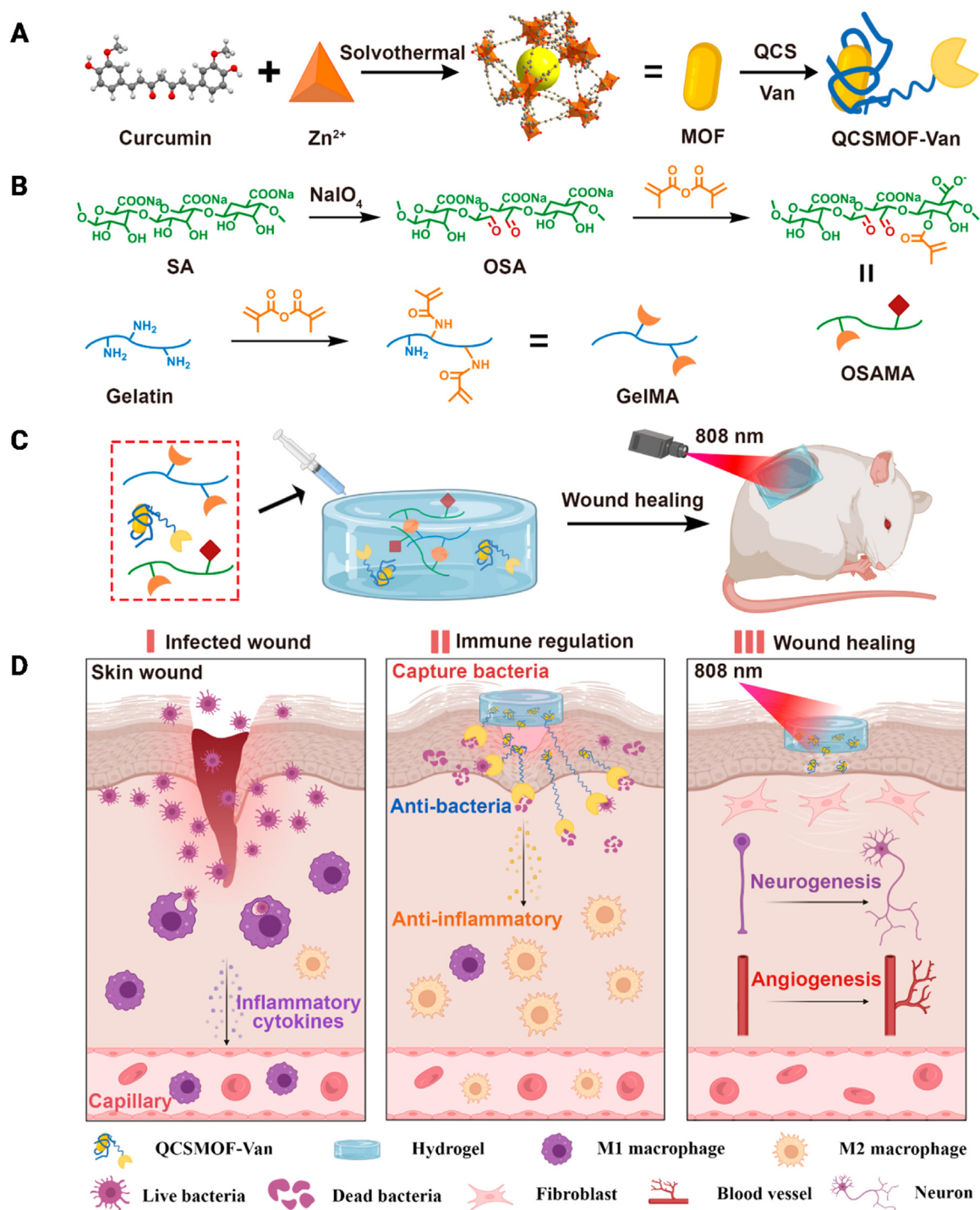
Fig. 9 – (A) Assembly of Zn-MOF with curcumin as Organic Ligand, subsequently modifying with QCS. (B) The composition of the IPN network. (C) The application diagram of composite hydrogel. (D) The efficacy and mechanism of composite hydrogel. Reproduced from [83] with permission from American Chemical Society.

increased pore size and swelling rate, it can promote fluid diffusion and drug release [143]. At the same time, metal ions such as Zn^{2+} released due to MOF skeleton degradation can have synergistic effects with metformin [144]. Furthermore, it is worth mentioning that due to the high loading capacity of MOFs and their metal ion release characteristics *in vivo*, they may represent an ideal carrier for delivering disulfiram to tumor sites. This is supported by findings that the anticancer activity of disulfiram is highly dependent on the presence of metal ions, particularly copper ions [145]. In addition to chemical drugs, biological agents such as siRNA can achieve efficient loading in MOFs [114,146]. The encapsulation of hydrogel beads also protected MOF particles in the gastrointestinal environment. Furthermore, due to the
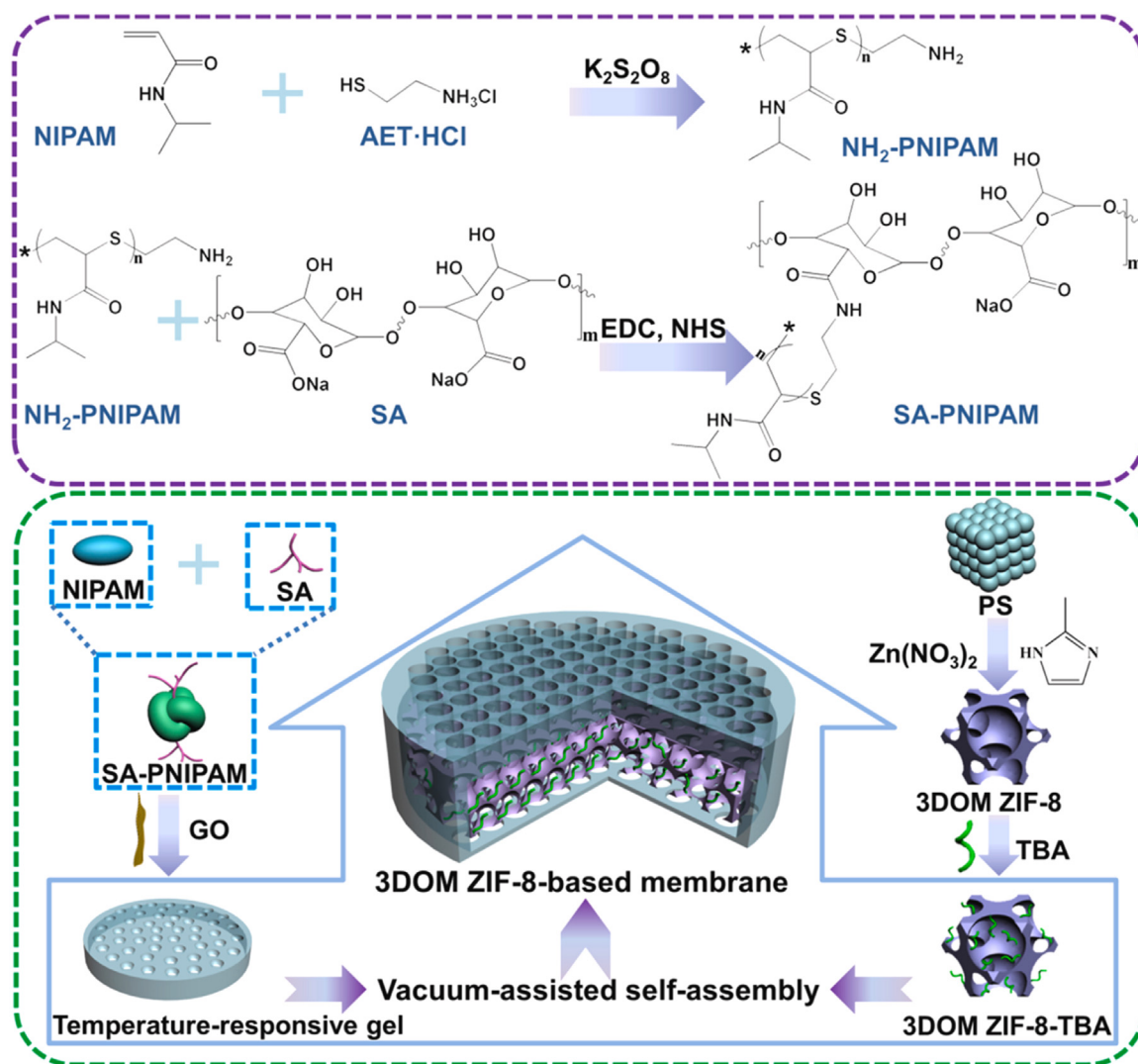
Fig. 10 – (A) Biomimetic synergetic antibacterial hydrogel, synergetic antibacterial, promotes wound healing in the whole process. Reproduced from [142] with permission from Elsevier. (B) Synthesis of biomimetic synergistic antibacterial hydrogel. Reproduced from [142] with permission from Elsevier.

degradation of the outer surface biomineralization layer in the acidic environment, the composite gel beads showed higher cell uptake and mucosal penetration. Moreover, the pH sensitivity of ZIF-8 could disrupt endosomes and help siRNA escape after cell uptake [146].

In addition, making appropriate improvements on the basis of traditional MOFs is very attractive for drug delivery. For example, a novel MOF (Cu-MOF-LDH)@Alg assembled on an Al-Cu double layered hydroxide substrate could achieve a drug encapsulation efficiency of up to 97.5%. That was because Cu-MOF-LDH provided high surface area and abundant active sites for drug adhesion, resulting in stronger interactions [112]. Similarly, adding some organic components such as GO would also provide additional adsorption sites for drugs and might enhance the bioavailability of nanocomposites [30]. In addition to the drug loading method, the size of the composite MOF crystal also affects the drug delivery. Research found that when there were small-sized crystals or a small amount of large-sized crystals in Alg, the drug release was lower and the sudden release situation was improved [97]. In this case,

Fig. 11 – Construction diagram and model structure of 3DOM ZIF-8. Reproduced from [115] with permission from Elsevier.

the crystals would be evenly distributed within the network structure, forming tortuous routes to delay drug release.

5.3. Other biomedical applications

Based on excellent enrichment and adsorption potential, there are also some interesting applications of MOFs@Alg composite gel, which are extracting specific substances from complex biological samples for testing or treatment. Hemodialysis is the most effective method for treating end-stage kidney disease, but traditional hemodialysis relies on a large amount of dialysate [147]. The MOFs@Alg provides some new ideas for miniaturized and simple dialysis devices. Specifically, filling Cu-Alg networks with moderate UiO-66 for composite beads, its maximum adsorption capacity for creatinine reached 125.0 mg/g with one tenth of the amount of dialysate used [76]. Among them, various interactions were formed between UIO-66 crystals and Cu-Alg, which was beneficial for improving adsorption. Ulteriorly, the composite beads were introduced into thin-film comprising supernatant PVA as a separation layer removing toxin rapidly

and lower electrospun PAN layer as a supporting layer to favor the toxin diffusion. The composite film provides a universal template for lightweight or miniaturized dialysis. Researches suggested that due to its excellent mass transfer performance, the membrane outperforms the bead matrix in terms of rapid protein capture [148]. To this end, after undergoing reasonable modification, the MOFs@Alg membrane as a temperature sensitive intelligent gating for the enrichment of low abundance protein thrombin was manufactured [115]. Its excellent selectivity came from the modification of ZIF-8 by thrombin aptamer (TBA) (3DOM ZIF-8), while its temperature sensitivity was attributed to the successful grafting of N-isopropylacrylamide onto SA (SA-PNIPAM) (Fig. 11). Interestingly, the prepared membrane could achieve the removal of high abundance proteins while enriching thrombin. Specifically, under a controlled temperature system, utilizing the characteristic that the channel size of temperature sensitive polymers gradually increased with elevating temperature, the proteins with special size scopes in biological samples could pass through the membrane based on the size exclusion effect.

6.   Conclusion and perspective

Taken together, based on the gelling mechanism of SA with diverse cation ions, this review has provided comprehensive insights into the different preparation routes, improvement strategies and various available forms of MOFs@Alg as well as the prospective applications through a detailed examination of the current relative literature. In this paper, the microscopic mechanism and influencing factors of composite gel formed by three preparation routes are described in detail, and their advantages and disadvantages are also pointed out. Among them, due to the difference in coordination ability and affinity with SA, the metal ions used for coordination and crosslinking are the main driving factors in the in-situ growth of composite gel. At the same time, affected by different preparation methods and reaction conditions such as temperature, solvent, pH and additives, the composite gel finally showed a variety of microstructures, crystal loading rates and physicochemical properties. Although it is difficult to accurately control the internal structure of the composite gel, maximizing the understanding of the accessible influencing factors is advantageous. What is more, the elaborate design strategies including IPN introduction, functional groups and crystal modified, physical doping, targeted modification and application form improvement are all described in order to obtain more ideal composite gels to meet diverse requirements. Finally, this article sheds light on the application of biomedical fields such as antibacterial, wound healing, drug delivery, and biological sample processing. Using gel as tunable platforms, all of them take full advantage of special characteristics of MOFs such as photothermal ability, highly designable and abundant binding sites in both porous crystal and flexible gel.

Despite the huge achievements and researches have been achieved, there is still a long way with challenges for MOFs@Alg towards better performance and practical application. Undoubtedly, a sophisticated composite gel with synergistic effects is promising, especially for biomedical applications. This depends on the synergy between SA based gels and MOFs based fillers. SA coating significantly improves the biocompatibility and stability of MOFs, simultaneously expanding their application forms. Nevertheless, the interaction between biopolymers and MOFs may be more complex than expected, especially in the process of in-situ growth. The surface charge, dispersion, crystallinity, and porosity of MOFs will be changed, which is further reflected in the particle size, shape, low load, and uniformity of distribution in the gel network of MOF crystals that are difficult to accurately control during the synthesis of composite gel. These will inevitably affect the loading of drugs, so it is meaningful to analyze and explore the relevant micro-mechanisms and influencing factors in this article. A suitable reaction system may break these barriers. However, describing and quantifying these changes is difficult and may require rigorous analysis and comparison with bare MOFs. In addition, due to biosafety considerations, the available types of MOFs and crosslinked ions are very limited, hence it is meaningful to focus attention on the development of new MOFs with high biocompatibility. Besides, the rational components regulation of MOFs such as inorganic components doping, using novel bio-organic ligands, or ligand functionalization methods may contribute to the improvement of MOFs' performance, chemical, and biological behavior. However, the precise theoretical experiments cannot predict the exact physicochemical and biological properties of the final composite, especially in the case of biopolymer SA participation in the crystal formation of MOFs. A complete library of organic-inorganic-ligands components or calculations based on density functional theory may offer a possibility to predictive systems for subsequent performance. Furthermore, research of the hydrogel composite system mainly stays at the laboratory level accompanied by the early exploring stages of evaluation index standards and large-scale production, further hindering the evaluation of composite safety and effectiveness in large experimental animals and clinical settings. Future research oriented biomedical applications should not only focus on carrier design but also comprehend complex interactions between MOFs@Alg composite gels and biological systems, especially the pharmacokinetics, metabolism, distribution, and potential side effects after crystal collapse. In brief, the analytical investigation on the current art state of MOFs@Alg provides more room for progression. Although there are many problems to be solved, its bright prospects can be foreseen.

Conflicts of interest

The authors declare that there is no conflicts of interest.

Acknowledgements

References

[1] Zhang YK, Lv JT, Zhao JH, Ling GX, Zhang P. A versatile GelMA composite hydrogel: designing principles, delivery forms and biomedical applications. Eur Polym J 2023;197:112370.

[2] Xu JQ, Zhang MY, Du WZ, Zhao JH, Ling GX, Zhang P. Chitosan-based high-strength supramolecular hydrogels for 3D bioprinting. Int J Biol Macromol 2022;219:545–57.

[3] Schmidt BVKJ. Multicompartment hydrogels. Macromol Rapid Comm 2022;43(7):e2100895.

[4] Zhang Y, Tan Y, Lao J, Gao H, Yu J. Hydrogels for flexible electronics. ACS Nano 2023;17(11):9681–93.

[5] Yang Z, He Y, Ma Y, Li L, Wang Y. A reversible adhesive hydrogel tape. Adv Funct Mater 2023;33(12):2213150.

[6] Yang Y, Luo S, Peng X, Zhao T, He Q, et al. An intra-articular injectable phospholipids-based gel for the treatment of rheumatoid arthritis. Asian J Pharm Sci 2023;18(1):100777.

[7] Sikorski P, Mo F, Skjak-Braek G, Stokke BT. Evidence for egg-box-compatible interactions in calcium-alginate gels from fiber X-ray diffraction. Biomacromolecules 2007;8(7):2098–103.

[8] Lai WF, Huang E, Lui KH. Alginate-based complex fibers with the Janus morphology for controlled release of co-delivered drugs. Asian J Pharm Sci 2021;16(1):77–85.

[9] Lee DW, Didriksen T, Olsbye U, Blom R, Grande CA. Shaping of metal-organic framework UiO-66 using alginates: effect of operation variables. Sep Purif Technol 2020;235:116182.

[10] Stankovic B, Jovanovic J, Adnadevic B. The kinetics of non-isothermal dehydration of equilibrium swollen Ca-alginate hydrogel. J Therm Anal Calorim 2020;142(5):2123–9.

[11] Hu CH, Lu W, Mata A, Nishinari K, Fang YP. Ions-induced gelation of alginate: mechanisms and applications. Int J Biol Macromol 2021;177:578–88.

[12] Zhang X, Wang L, Weng L, Deng B. Strontium ion substituted alginate-based hydrogel fibers and its coordination binding model. J Appl Polym Sci 2020;137(16):48571.

[13] Caccavo D, Ström A, Larsson A, Lamberti G. Modeling capillary formation in calcium and copper alginate gels. Mat Sci Eng C-Mater 2016;58:442–9.

[14] Li Y, Zhang X, Chen X, Tang K, Meng Q, et al. Zeolite imidazolate framework membranes on polymeric substrates modified with poly(vinyl alcohol) and alginate composite hydrogels. ACS Appl Mater Inter 2019;11(13):12605–12.

[15] Omer AM, Abd El-Monaem EM, El-Subruiti GM, Abd El-Latif MM, Eltaweil AS. Fabrication of easy separable and reusable MIL-125(Ti)/MIL-53(Fe) binary MOF/CNT/alginate composite microbeads for tetracycline removal from water bodies. Sci Rep 2021;11(1):23818.

[16] Li J, Wang X, Liu P, Liu X, Li L, Li J. Shaping of metal-organic frameworks through a calcium alginate method towards ethylene/ethane separation. Chinese J Chem Eng 2022;42:17–24.

[17] Sun W, Zhao X, Webb E, Xu G, Zhang W, Wang Y. Advances in metal–organic framework-based hydrogel materials: preparation, properties and applications. J Mater Chem A 2023;11(5):2092–127.

[18] Dong HXL, Shui W. Metal organic framework-based antibacterial agents and their underlying mechanisms. Chem Soc Rev 2022;51(16):7138–69.

[19] Zhao L, Wang B, Wang C, Fan D, Liu X, et al. Dual-strategy ECL biosensor based on rare Eu(II,III)-MOF as probe with antenna effect and sensitization for CYFRA 21-1 trace analysis. Sensor Actuat B-Chem 2023;377.

[20] Li J, Fu Z, Liu Y. Encapsulation of liquid metal nanoparticles inside metal-organic frameworks for hydrogel-integrated dual functional biotherapy. Chem Eng J 2023;457:141302.

[21] Deole D. Metal-organic frameworks for carbon dioxide capture: using sustainable synthesis routes. Curr Org Synth 2022;19(5):673–84.

[22] Wang C, Wang J, Pan X, Yu S, Chen M, et al. Reversing ferroptosis resistance by MOFs through regulation intracellular redox homeostasis. Asian J Pharm Sci 2023;18(1):88–98.

[23] Hammi N, El Hankari S, Katir N, Marcotte N, Draoui K, et al. Polysaccharide templated biomimetic growth of hierarchically porous metal-organic frameworks. Micropor Mesoporous Mat 2020;306:110429.

[24] Wang L, Li Z, Wang Y, Gao M, He T, et al. Surface ligand-assisted synthesis and biomedical applications of metal-organic framework nanocomposites. Nanoscale 2023;15(25):10529–57.

[25] Cui A-Q, Wu X-Y, Ye J-B, Song G, Chen D-Y, et al. Two-in-one" dual-function luminescent MOF hydrogel for onsite ultra-sensitive detection and efficient enrichment of radioactive uranium in water. J Hazard Mater 2023;448:130864.

[26] Chai Y, Zhang Y, Wang L, Du Y, Wang B, et al. In situ one-pot construction of MOF/hydrogel composite beads with enhanced wastewater treatment performance. Sep Purif Technol 2022;295:121225.

[27] Nabipour H, Rohani S. Green synthesis of pH-responsive metal-organic frameworks for delivery of diclofenac sodium. IEEE T Nanobiosci 2023:1.

[28] Gao X, Hai X, Baigude H, Guan W, Liu Z. Fabrication of functional hollow microspheres constructed from MOF shells: promising drug delivery systems with high loading capacity and targeted transport. Sci Rep 2016;6(1):37705.

[29] Ashouri Sharafshadeh S, Mehdinavaz Aghdam R, Akhlaghi P, Heirani-Tabasi A. Amniotic membrane/silk fibroin-alginate nanofibrous scaffolds containing Cu-based metal organic framework for wound dressing. Int J Polym Mater 2024;73(1):33–44.

[30] Rabiee N, Bagherzadeh M, Jouyandeh M, Zarrintaj P, Saeb MR, et al. Natural polymers decorated MOF-MXene nanocarriers for co-delivery of doxorubicin/pCRISPR. ACS Appl Bio Mater 2021;4(6):5106–21.

[31] Vahed TA, Naimi-Jamal MR, Panahi L. Alginate-coated ZIF-8 metal-organic framework as a green and bioactive platform for controlled drug release. J Drug Deliv Sci Tec 2019;49:570–6.

[32] Guan J, Feng X, Zeng Q, Li Z, Liu Y, et al. A new in situ prepared MOF-natural polymer composite electrolyte for solid lithium metal batteries with superior high- rate capability and long-term cycling stability at ultrahigh current density. Adv Sci 2023;10(3):2203916.

[33] Chen B, Li Y, Du Q, Pi X, Wang Y, et al. Effective removal of tetracycline from water using copper alginate @ graphene oxide with in-situ grown MOF-525 composite: synthesis, characterization and adsorption mechanisms. NanomaTerials-Basel 2022;12(17):2897.

[34] Zhao Y, Wang Y, Wang M, Liang N, Li Z. Bio-mediated MOF-derived core-shell flame retardant: towards styrene-butadiene-styrene asphalt with enhanced flame safety and pavement performance. Constr Build Mater 2023;392:131408.

[35] Yu R, Wu Z. The adsorption property of in-situ synthesis of MOF in alginate gel for ofloxacin in the wastewater. Environ Technol 2023;44(16):2395–406.

[36] Wang Y, Peng H, Wang H, Zhang M, Zhao W, Zhang Y. In-situ synthesis of MOF nanoparticles in double-network hydrogels for stretchable adsorption device. Chem Eng J 2022;450:138216.

[37] Kong Y, Zhuang Y, Han K, Shi B. Enhanced tetracycline adsorption using alginate-graphene-ZIF67 aerogel. Colloid Surface A 2020;588:124360.

[38] Qin L, Ru R, Mao J, Meng Q, Fan Z, et al. Assembly of MOFs/polymer hydrogel derived Fe_3O_4-CuO@hollow carbon spheres for photochemical oxidation: freezing replacement for structural adjustment. Appl Catal B-Environ 2020;269:118754.

[39] Park SH, Kim K, Lim JH, Lee SJ. Selective lithium and magnesium adsorption by phosphonate metal-organic framework-incorporated alginate hydrogel inspired from lithium adsorption characteristics of brown algae. Sep Purif Technol 2019;212:611–18.

[40] Lim J, Lee EJ, Choi JS, Jeong NC. Diffusion control in the in situ synthesis of iconic metal-organic frameworks within an ionic polymer matrix. ACS Appl Mater Inter 2018;10(4):3793–800.

[41] Liu W, Erol O, Gracias DH. 3D printing of an in situ grown MOF hydrogel with tunable mechanical properties. ACS Appl Mater Inter 2020;12(29):33267–75.

[42] Zhuang Y, Kong Y, Wang X, Shi B. Novel one step preparation of a 3D alginate based MOF hydrogel for water treatment. New J Chem 2019;43(19):7202–8.

[43] Zhang T, Li P, Ding S, Wang X. High-performance TFNC membrane with adsorption assisted for removal of Pb(II) and other contaminants. J Hazard Mater 2022;424:127742.

[44] Narayanan RP, Melman G, Letourneau NJ, Mendelson NL, Melman A. Photodegradable iron(III) cross-linked alginate gels. Biomacromolecules 2012;13(8):2465–71.

[45] Leong JY, Lam WH, Ho KW, Voo WP, Lee MFX, et al. Advances in fabricating spherical alginate hydrogels with controlled particle designs by ionotropic gelation as encapsulation systems. Particuology 2016;24:44–60.

[46] Mørch YA, Donati I, Strand BL, Skjåk-Braek G. Effect of Ca^{2+}, Ba^{2+}, and Sr^{2+} on alginate microbeads. Biomacromolecules 2006;7(5):1471–80.

[47] Lu L, Liu X, Tong Z. Critical exponents for sol-gel transition in aqueous alginate solutions induced by cupric cations. Carbohyd Polym 2006;65(4):544–51.

[48] Rodrigues JR, Lagoa R. Copper ions binding in Cu-alginate gelation. J Carbohyd Chem 2006;25(2–3):219–32.

[49] Lee KY, Mooney DJ. Alginate: properties and biomedical applications. Prog Polym Sci 2012;37(1):106–26.

[50] Zhu H, Zhang Q, Zhu SP. Alginate hydrogel: a shapeable and versatile platform for in situ preparation of metal-organic framework-polymer composites. ACS Appl Mater Inter 2016;8(27):17395–401.

[51] Deramos CM, Nauss JL, Stout BE, Irwin AE. 13C NMR and molecular modeling studies of alginic acid binding with alkaline earth and lanthanide metal ions. Inorg Chim Acta 1997;256(1):69–75.

[52] Chen YF, Teng JH, Liao BQ, Li RJ, Lin HJ. Molecular insights into the impacts of iron(III) ions on membrane fouling by alginate. Chemosphere 2020;242:125232.

[53] Li M, Huang W, Tang B, Fang Q, Ling X, Lv A. Characterizations and n-Hexane vapor adsorption of a series of MOF/alginates. Ind Eng Chem Res 2020;59(42):18835–43.

[54] Dodero A, Vicini S, Castellano M. Depolymerization of sodium alginate in saline solutions via ultrasonic treatments: a rheological characterization. Food Hydrocolloid 2020;109(0):106128.

[55] Wang Y, Peng H, Zhang Y. Concentration gradient induced in situ formation of MOF tubes. Chem Commun 2021;57(59):7300–3.

[56] Ahmadi M, Ayyoubzadeh SM, Ghorbani-Bidkorbeh F, Shahhosseini S, Dadashzadeh S, et al. An investigation of affecting factors on MOF characteristics for biomedical applications: a systematic review. Heliyon 2021;7(4): e06914.

[57] Shu J, Niu Q, Wang N, Nie J, Ma G. Alginate derived Co/N doped hierarchical porous carbon microspheres for efficient oxygen reduction reaction. Appl Surf Sci 2019;485:520–8.

[58] Wang Z, Hu SG, Yang J, Liang AJ, Li YS, et al. Nanoscale zr-based MOFs with tailorable size and introduced mesopore for protein delivery. Adv Funct Mater 2018;28(16):1707356.

[59] Dehghani S, Alam NR, Shahriarian S, Mortezazadeh T, Haghgoo S, et al. The effect of size and aspect ratio of Fe-MIL-88B-NH metal-organic frameworks on their relaxivity and contrast enhancement properties in MRI: in vitro and in vivo studies. J Nanopart Res 2018;20(10).

[60] Devic T, Serre C. High valence 3p and transition metal based MOFs. Chem Soc Rev 2014;43(16):6097–115.

[61] Ritter S. Hard and soft acids and bases. Chem Eng News 2003;81(7):50.

[62] Bunzen H. Chemical stability of metal-organic frameworks for applications in drug delivery. Chemnanomat 2021;7(9):998–1007.

[63] Lin Y, Wang Q, Huang Y, Du J, Cheng Y, et al. Design of amphoteric MOFs-cellulose based composite for wastewater remediation: adsorption and catalysis. Int J Biol Macromol 2023;247:125559.

[64] Khan AAP, Patil MB, Rathod LP, Vader SG, Raizada P, et al. Polymer membranes of zeolitic imidazole framework-8 with sodium alginate synthesized from ZIF-8 and their application in light gas separation. Polymers 2023;15(4):1011.

[65] Shang M, Peng X, Zhang J, Liu X, Yuan Z, et al. Sodium alginate-based carbon aerogel-supported ZIF-8-derived porous carbon as an effective adsorbent for methane gas. ACS Appl Mater Inter 2023;15(11):14634–42.

[66] Xiao S, Li M, Cong H, Wang L, Li X, Zhang W. Preparation of highly porous thiophene-containing DUT-68 beads for adsorption of CO_2 and iodine vapor. Polymers 2021;13(23):4075.

[67] Song Y, Wang N, Yang LY, Wang YG, Yu D, Ouyang XK. Ouyang X-k. Facile fabrication of ZIF-8/calcium alginate microparticles for highly efficient adsorption of Pb(II) from aqueous solutions. Ind Eng Chem Res 2019;58(16):6394–401.

[68] Wu C, Dan Y, Tian D, Zheng Y, Wei S, Xiang D. Facile fabrication of MOF(Fe)@alginate aerogel and its application for a high-performance slow-release N-fertilizer. Int J Biol Macromol 2020;145:1073–9.

[69] Jia W, Fan R, Zhang J, Zhu K, Gai S, et al. Smart MOF-on-MOF hydrogel as a simple rod-shaped core for visual detection and effective removal of pesticides. Small 2022;18(19):e2201510.

[70] Jia W, Fan R, Zhang J, Zhu K, Gai S, et al. Home-made multifunctional auxiliary device for in-situ imaging detection and removal of quinclorac residues through MOF decorated gel refills. Chem Eng J 2022;450:138303.

[71] Liu D, Gu W, Zhou W, Xu Y, He W, et al. Magnetic e/carbon/sodium alginate hydrogels for efficient degradation of norfloxacin in simulated wastewater. J Clean Prod 2022;369:133239.

[72] Pei R, Fan L, Zhao F, Xiao J, Yang Y, et al. 3D-Printed metal-organic frameworks within biocompatible polymers as excellent adsorbents for organic dyes removal. J Hazard Mater 2020;384:121418.

[73] Lee SJ, Hann T, Park SH. Seawater desalination using MOF-incorporated Cu-based alginate beads without energy consumption. ACS Appl Mater Inter 2020;12(14):16319–26.

[74] Bai Z, Liu Q, Zhang H, Yu J, Chen R, et al. Anti-biofouling and water-stable balanced charged metal organic framework-based polyelectrolyte hydrogels for extracting uranium from seawater. ACS Appl Mater Inter 2020;12(15):18012–22.

[75] Gwon K, Lee S, Kim Y, Choi J, Kim S, et al. Construction of a bioactive copper-based metal organic framework-embedded dual-crosslinked alginate hydrogel for antimicrobial applications. Int J Biol Macromol 2023;242:124840.

[76] Ding S, Li P, Zhang T, Wang X. Coordination of copper ion crosslinked composite beads with enhanced toxins adsorption and thin-film nanofibrous composite membrane for realizing the lightweight hemodialysis. Adv Fiber Mater 2022;4(3):556–70.

[77] Mondino G, Spjelkavik AI, Didriksen T, Krishnamurthy S, Stensrod RE, et al. Production of MOF adsorbent spheres and comparison of their performance with zeolite 13X in a moving-bed TSA process for postcombustion CO_2 capture. Ind Eng Chem Res 2020;59(15):7198–211.

[78] Wei C-M, Feng C-Y, Li S, Zou Y, Yang Z. Mushroom tyrosinase immobilized in metal-organic frameworks as an excellent catalyst for both catecholic product synthesis and phenolic wastewater treatment. J Chem Technol Biot 2022;97(4):962–72.

[79] Sha H, Yan B. A pH-responsive Eu(III) functionalized metal-organic framework hybrid luminescent film for amino acid sensing and anti-counterfeiting. J Mater Chem C 2022;10(19):7633–40.

[80] Yang S, Peng L, Syzgantseva OA, Trukhina O, Kochetygov I, et al. Preparation of highly porous metal-organic framework beads for metal extraction from liquid streams. J Am Chem Soc 2020;142(31):13415–25.

[81] Ma H, Yang Y, Yin F, Zhang X-F, Qiu J, Yao J. Integration of thermoresponsive MIL-121 into alginate beads for

efficient heavy metal ion removal. J Clean Prod 2022;333:130229.

[82] Luo Z, Chen H, Wu S, Yang C, Cheng J. Enhanced removal of bisphenol a from aqueous solution by aluminum-based MOF/sodium alginate-chitosan composite beads. Chemosphere 2019;237:124493.

[83] Huang K, Liu W, Wei W, Zhao Y, Zhuang P, et al. Photothermal hydrogel encapsulating intelligently bacteria-capturing bio-MOF for infectious wound healing. ACS Nano 2022;16(11):19491–508.

[84] Loo HL, Goh BH, Lee LH, Chuah LH. Application of chitosan-based nanoparticles in skin wound healing. Asian J Pharm Sci 2022;17(3):299–332.

[85] Guibal E. Interactions of metal ions with chitosan-based sorbents:a review. Sep Purif Technol 2004;38(1):43–73.

[86] Ren X, Yang C, Zhang L, Li S, Shi S, et al. Copper metal-organic frameworks loaded on chitosan film for the efficient inhibition of bacteria and local infection therapy. Nanoscale 2019;11(24):11830–8.

[87] Hsieh Y-J, Zou C, Chen J-J, Lin L-C, Kang D-Y. Pillared-bilayer metal-organic framework membranes for dehydration of isopropanol. Micropor Mesoporous Mat 2021;326:1387–811.

[88] Xu N, Zhang MY, Xu WX, Ling GX, Yu J, Zhang P. Swellable PVA/PVP hydrogel microneedle patches for the extraction of interstitial skin fluid toward minimally invasive monitoring of blood glucose level. Analyst 2022;147(7):1478–91.

[89] Lee SJ, Lim HW, Park SH. Adsorptive seawater desalination using MOF-incorporated Cu-alginate/PVA beads: ion removal efficiency and durability. Chemosphere 2021;268:128797.

[90] Zhang G, Chen H, Yang G, Fu H. Preparation of in situ ZIF-9 grown on sodium alginate/polyvinyl alcohol hydrogels for enhancing Cu (II) adsorption from aqueous solutions. J Inorg Organomet P 2022;32(12):4576–88.

[91] Alkas TR, Purnomo AS, Pratiwi AN, Nurwijayanti Y, Ediati R, et al. Immobilization of UiO-66/Brown-rot fungi (BRF) in PVA-SA matrix and its performance for methylene blue decolorization. Mater Today Chem 2023;29:101411.

[92] Musarurwa H, Tavengwa NT. Application of polysaccharide-based metal organic framework membranes in separation science. Carbohyd Polym 2022;275:118743.

[93] Zhao H, Sun J, Du Y, Zhang M, Yang Z, et al. In-situ immobilization of CuMOF on sodium alginate/chitosan/cellulose nanofibril composite hydrogel for fast and highly efficient removal of Pb2+from aqueous solutions. J Solid State Chem 2023;322:123928.

[94] du Poset AM, Lerbret A, Boue F, Zitolo A, Assifaoui A, Cousin F. Tuning the structure of galacturonate hydrogels: external gelation by Ca, Zn, or Fe cationic cross-Linkers. Biomacromolecules 2019;20(7):2864–72.

[95] Yan YZ, An QD, Xiao ZY, Zheng W, Zhai SG. Flexible core-shell/bead-like alginate@PEI with exceptional adsorption capacity, recycling performance toward batch and column sorption of Cr(VI). Chem Eng J 2017;313:475–86.

[96] Lu Y, Yu L, Zhang S, Su P, Li X, et al. Dual-functional fluorescent metal-organic framework based beads for visual detection and removal of oxytetracycline in real aqueous solution. Appl Surf Sci 2023;625:157202.

[97] de Lima HHC, da Silva CTP, Kupfer VL, JdC Rinaldi, Kioshima ES, et al. Synthesis of resilient hybrid hydrogels using UiO-66 MOFs and alginate (hydroMOFs) and their effect on mechanical and matter transport properties. Carbohyd Polym 2021;251:116977.

[98] Alvares E, Tantoro S, Julius C, Cheng K-C, Soetaredjo FE, et al. Preparation of MIL100/MIL101-alginate composite beads for selective phosphate removal from aqueous solution. Int J Biol Macromol 2023;231:123322.

[99] Ali I, Wan P, Raza S, Peng C, Tan X, et al. Development of novel MOF-mixed matrix three-dimensional membrane capsules for eradicating potentially toxic metals from water and real electroplating wastewater. Environ Res 2022;215:113945.

[100] Xu WQ, Wu Y, Jiao L, Sha M, Cai XL, et al. Protein trap-engineered metal-organic frameworks for advanced enzyme encapsulation and mimicking. Nano Res 2023;16(2):3364–71.

[101] Yang W, Yu T, Sun L, Liu Q, Fei Z, et al. Pore-expanded UiO-66 pellets for efficient bisphenol A adsorption. Chem Eng J 2023;455:140843.

[102] Pandi K, Prabhu SM, Ahn Y, Park CM, Choi J. Design and synthesis of biopolymer-derived porous graphitic carbon covered iron-organic frameworks for depollution of arsenic from waters. Chemosphere 2020;254:126769.

[103] Eltaweil AS, Mamdouh IM, Abd El-Monaem EM, El-Subruiti GM. Highly efficient removal for methylene blue and Cu^{2+} onto UiO-66 metal-organic framework/carboxylated graphene oxide-incorporated sodium alginate beads. Acs Omega 2021;6(36):23528–41.

[104] Kim N, Cha B, Yea Y, Njaramba LK, Vigneshwaran S, et al. Effective sequestration of tetracycline and ciprofloxacin from aqueous solutions by Al-based metal organic framework and reduced graphene oxide immobilized alginate biosorbents. Chem Eng J 2022;450:138068.

[105] Ghani AA, Devarayapalli KC, Kim B, Lim Y, Kim G, et al. Sodium-alginate-laden MXene and MOF systems and their composite hydrogel beads for batch and fixed-bed adsorption of naproxen with electrochemical regeneration. Carbohyd Polym 2023;318:121098.

[106] Oh JY, Choi E, Jana B, Go EM, Jin E, et al. Protein-precoated surface of metal-organic framework nanoparticles for targeted delivery. Small 2023;19(22):e2300218.

[107] Figueroa-Quintero L, Villalgordo-Hernández D, Delgado-Marín JJ, Narciso J, Velisoju VK, et al. Post-synthetic surface modification of metal-organic frameworks and their potential applications. Small Methods 2023;7(4):1.

[108] Ferreira LF, Picco AS, Galdino FE, Albuquerque LJC, Berret JF, Cardoso MB. Nanoparticle-protein interaction: demystifying the correlation between protein corona and aggregation phenomena. ACS Appl Mater Inter 2022;14(25):28559–69.

[109] Zhao Z, Li X, Wang Y, Liu C, Ling G, Zhang P. Biomimetic platelet-camouflaged drug-loaded polypyrrole for the precise targeted antithrombotic therapy. J Nanobiotechnol 2023;21(1):439.

[110] Yao Q, Ye JY, Chen YH, Huang LH, Sun LN, et al. Modulation of glucose metabolism through macrophage-membrane-coated metal-organic framework nanoparticles for triple-negative breast cancer therapy. Che Eng J 2024;480:148069.

[111] Zhang J, Chen C, Li AN, Jing WQ, Sun P, et al. Immunostimulant hydrogel for the inhibition of malignant glioma relapse post-resection. Nat Nanotechnol 2021;16(5):538–48.

[112] Karimi S, Rasuli H, Mohammadi R. Facile preparation of pH-sensitive biocompatible alginate beads havening layered double hydroxide supported metal-organic framework for controlled release from doxorubicin to breast cancer cells. Int J Biol Macromol 2023;234:123538.

[113] Zhong N, Gao R, Shen Y, Kou X, Wu J, et al. Enzymes-encapsulated defective metal-organic framework hydrogel coupling with a smartphone for a portable glucose biosensor. Anal Chem 2022;94(41):14385–93.

[114] Gao M, Yang C, Wu C, Chen Y, Zhuang H, et al. Hydrogel-metal-organic-framework hybrids mediated efficient oral delivery of siRNA for the treatment of ulcerative colitis. J Nanobiotechnol 2022;20(1):404.

[115] Lin Y, Xu Y, Xing Y, Liu N, Chen X. Three-dimensional ordered macroporous MOF-based smart gating membrane with size screening effect and aptamer specificity for highly efficient thrombin isolation. J Membrane Sci 2023;665:121132.

[116] Feng S, Tang Q, Xu Z, Huang K, Li H, Zou Z. Development of novel Co-MOF loaded sodium alginate based packaging films with antimicrobial and ammonia-sensitive functions for shrimp freshness monitoring. Food Hydrocolloid 2023;135:108193.

[117] Dai X, Li X, Wang XL. Morphology controlled porous poly(lactic acid)/zeolitic imidazolate framework-8 fibrous membranes with superior PM2.5 capture capacity. Chem Eng J 2018;338:82–91.

[118] Muñoz-Ruíz Abraham, Escobar-García Diana M, Quintana Mildred. Amaury Pozos-Guillén, Flores H. Synthesis and characterization of a new collagen-alginate aerogel for tissue engineering. J Nanomater 2019;2019(1):1–10.

[119] Gorshkova N, Brovko O, Palamarchuk I, Bogolitsyn K, Ivakhnov A. Preparation of bioactive aerogel material based on sodium alginate and chitosan for controlled release of levomycetin. Polym Advan Technol 2021;32(9):3474–82.

[120] Bauleth-Ramos T, Shih TY, Shahbazi MA, Najibi AJ, Mao AS, et al. Acetalated dextran nanoparticles loaded into an injectable alginate cryogel for combined chemotherapy and cancer vaccination. Adv Funct Mater 2019;29(35): 1903686.

[121] Du A, Zhou B, Zhang ZH, Shen J. A Special material or a new state of matter: a review and reconsideration of the aerogel. Materials 2013;6(3):941–68.

[122] El-Naggar ME, Othman SI, Allam AA, Morsy OM. Synthesis, drying process and medical application of polysaccharide-based aerogels. Int J Biol Macromol 2020;145(0):1115–28.

[123] Han JQ, Zhou CJ, Wu YQ, Liu FY, Wu QL. Self-assembling behavior of cellulose nanoparticles during freeze-drying: effect of suspension concentration, particle size, crystal structure, and surface charge. Biomacromolecules 2013;14(5):1529–40.

[124] Fan Y, Liang H, Jian M, Liu R, Zhang X, et al. Removal of dimethylarsinate from water by robust NU-1000 aerogels: impact of the aerogel materials. Chem Eng J 2023;455:140387.

[125] Kong Y, Han K, Zhuang Y, Shi B. Facile Synthesis of MOFs-templated carbon aerogels with enhanced tetracycline adsorption performance. Water 2022;14(3):504.

[126] Li Q, Ying Y, Tao Y, Li H. Assemblable carbon fiber/metal-organic framework monoliths for energy-efficient atmospheric water harvesting. ind eng chem res 2022;61(3):1344–54.

[127] Zhang W, Wang B, Xiang G, Jiang T, Zhao X. Photodynamic alginate Zn-MOF thermosensitive hydrogel for accelerated healing of infected wounds. ACS Appl Mater Inter 2023;15(19):22830–42.

[128] Zhang M, Wang G, Wang D, Zheng Y, Li Y, et al. Ag@MOF-loaded chitosan nanoparticle and polyvinyl alcohol/sodium alginate/chitosan bilayer dressing for wound healing applications. Int J Biol Macromol 2021;175:481–94.

[129] Gwon K, Han I, Lee S, Kim Y, Lee DN. Novel metal-organic framework-based photocrosslinked hydrogel system for efficient antibacterial applications. ACS Appl Mater Inter 2020;12(18):20234–42.

[130] Pettinari C, Pettinari R, Di Nicola C, Tombesi A, Scuri S, Marchetti F. Antimicrobial MOFs. Coordin Chem Rev 2021;446:0010–8545.

[131] Fan W, Huang P, Chen X. Overcoming the Achilles' heel of photodynamic therapy. Chem Soc Rev 2016;45(23):6488–519.

[132] Kadiyala U, Kotov N, VanEpps J. Antibacterial metal oxide nanoparticles: challenges in interpreting the literature. Curr Pharm Design 2018;24(8):896–903.

[133] Gupta B, Papke JB, Mohammadkhah A, Day DE, Harkins AB. Effects of chemically doped bioactive borate glass on neuron regrowth and regeneration. Ann Biomed Eng 2016;44(12):3468–77.

[134] Chen RJ, Jiang ZW, Cheng YF, Ye JY, Li SZ, et al. Multifunctional iron-apigenin nanocomplex conducting photothermal therapy and triggering augmented immune response for triple negative breast cancer. Int J Pharmaceut 2024;655:124016.

[135] Cheng Y, Wen C, Sun YQ, Yu H, Yin XB. Mixed-metal MOF-derived hollow porous nanocomposite for trimodality imaging guided reactive oxygen species-augmented synergistic therapy. Adv Funct Mater 2021;31(37):2104378.

[136] Yang J, Yang YW. Metal-organic frameworks for biomedical applications. Small 2020;16(10):1906846.

[137] Fan ZJ, Li J, Liu JL, Jiao HJ, Liu B. Anti-inflammation and joint lubrication dual effects of a novel hyaluronic acid/curcumin nanomicelle improve the efficacy of rheumatoid arthritis therapy. ACS Appl Mater Inter 2018;10(28):23595–604.

[138] Sheng LL, Zhang ZWB, Zhang Y, Wang ED, Ma B, et al. A novel "hot spring"-mimetic hydrogel with excellent angiogenic properties for chronic wound healing. Biomaterials 2021;264:120414.

[139] Qin L, Ling G, Peng F, Zhang F. Black phosphorus nanosheets and gemcitabine encapsulated thermo-sensitive hydrogel for synergistic photothermal-chemotherapy. J Colloid Interf Sci 2019;556:232–8.

[140] Chen G, Yu Y, Wu X, Wang G, Ren J, Zhao Y. Bioinspired multifunctional hybrid hydrogel promotes wound healing. Adv Funct Mater 2018;28(33):1801386.

[141] Liu H, Qu X, Tan H, Song J, Lei M, et al. Role of polydopamine's redox-activity on its pro-oxidant, radical-scavenging, and antimicrobial activities. Acta Biomater 2019;88:181–96.

[142] Wang Y, Qi W, Mao Z, Wang J, Zhao RC, Chen H. rPDAs doped antibacterial MOF-hydrogel: bio-inspired synergistic whole-process wound healing. Mater Today Nano 2023;23:100363.

[143] Tonnesen HH, Karlsen J. Alginate in drug delivery systems. Drug Dev Ind Pharm 2002;28(6):621–30.

[144] Oruc A, Oruc KY, Yanar K, Mengi M, Caglar A, et al. The role of glycogen synthase kinase-3β in the zinc-mediated neuroprotective effect of metformin in rats with glutamate neurotoxicity. Biol Trace Elem Res 2023;204:25–6.

[145] Shen XY, Sheng HX, Zhang Y, Dong X, Kou LF, et al. Nanomedicine-based disulfiram and metal ion co-delivery strategies for cancer treatment. Int J Pharm-X 2024;7:100248.

[146] Zhuang J, Gong H, Zhou JR, Zhang QZ, Gao WW, et al. Targeted gene silencing in vivo by platelet membrane-coated metal-organic framework nanoparticles. Sci Adv 2020;6(13).

[147] Koubaissy B, Toufaily J, Yaseen Z, Daou TJ, Jradi S, Hamieh T. Adsorption of uremic toxins over dealuminated zeolites. Adsorpt Sci Technol 2017;35(1–2):3–19.

[148] Dong J, Bruening ML. Functionalizing microporous membranes for protein purification and protein digestion. Annu Rev Anal Chem 2015;8(1):81–100.